animal was placed in the arm facing the center (Arm A) and was allowed to freely explore for an 8-minute test session without the reinforcement of food, water, or electric foot shock. An arm entry was defined as the entry of all four paws into one arm. The sequence of arm entries was manually recorded. Alternation behavior (actual alternations) was defined as consecutive entry into the three arms (i.e., Arm A to B to C). The maximum number of alternations was calculated by measuring the total number of arm entries minus 2, and the percentage of alternation behavior was calculated as (actual alternations/maximum alternations) × 100. Each mouse was tested four times with the experiment. The total number of arms entered during the sessions, which reflects locomotor activity, was also recorded. We took the average of 3–4 experiments or more.

2.9. Pathologically analysis

Tissues (brain, liver, kidney and testis) were dissected and fixed with a 4% formaldehyde neutral buffer solution (Wako Co., LTD, Osaka, Japan) and embedded in paraffin. The sliced sections were then stained with H&E, toluidine blue stain, and immunostaining against the mouse lysosomal marker, lysosomal-associated membrane protein 2 (Lamp2) [18,19]. Immunostaining was performed according to a procedure previously described [20]. Briefly, the sliced sections were made permeable with PBS (−) containing 0.1% Triton X-100, and the slides were blocked with peroxidase and locked with 3% H_2O_2 in methanol. They were then blocked with PBS containing 10% normal goat serum (Vector Laboratories, CA, USA). The tissues were incubated with the anti-LAMP2 rabbit polyclonal antibody (AnaSpec Inc., catalog # 54234, CA, USA,). Biotinylated anti-rabbit IgG (H + L) antibody (Vector Laboratories, CA, USA) in PBS was then applied, and the slides were serially stained with an avidin–biotin complex using the ABC elite kit (Vector Laboratories, CA, USA) with 3, 3′-diaminobenzidine as a chromogen. Counterstaining for cell nuclei was performed with Mayer hematoxylin.

3. Results

3.1. Iduronate-2-sulfate-deficient mice have a coarse face because of bone deformation

We studied the faces of the MPS II mice using X-ray computed tomography (CT) (Fig. 1A). The IDS-knockout, MPS II model mice exhibited a phenotype characterized by a coarse face, large round eyes, and a rounded nose when compared with the wild-type mice. Furthermore, the X-ray CT analysis showed hyperostosis and nose dysostosis in the MPS II mouse head. The walking footprint patterns

of the MPS II mice and the wild-type controls at 21 weeks of age are illustrated (Fig. 1B). Most wild-type mice walked in a straight line away from the investigator. By contrast, MPS II mice walked unsteadily and walked with a short-stepped gait that had approximately half the stride length of the wild-type mice.

3.2. Intraventricular administration of ERT for the MPS II murine model

The IDS enzyme was injected into the MPS II mouse (21 week old) lateral ventricle 4 times. Mouse body weights were measured during intraventricular ERT or administration of normal saline (Fig. 2A). Body weights in the intraventricular ERT group were similar to those in the control animals. Mice brains were divided into three regions (front cerebral, posterior cerebral, and cerebellum) (Fig. 2B). In the disease-control, MPS II mice, the frontal and posterior regions of the brain showed almost negligible IDS enzyme activity. In contrast, in the intraventricular ERT group, cerebral IDS enzyme activity increased approximately three-fold compared with the wild-type group. Additionally, IDS activity in the cerebellum was elevated to levels comparable to those in the wild-type group (Fig. 2C). The accumulation of total GAGs was measured in the brain. Although the total GAGs in the disease-control group was elevated, this elevation was inhibited in the three brain regions after treatment with IDS via intraventricular ERT (Fig. 2D). We analyzed IDS enzyme activity following IDS administration with intraventricular ERT not only in the brain but also in other tissues (eye, lung, heart, liver, kidney, spleen, and testis). A deficiency in IDS enzyme activity was also found in other tissues of the disease-control, MPS II mice. In the intraventricular ERT group, IDS enzyme activity was increased to levels comparable to those in the wild-type group (Fig. 2E).

3.3. Effects of treatment with multiple administrations of IDS via intraventricular ERT for young adult MPS II mice

3.3.1. Analysis of alternation behavior and learning with the Y-maze test in MPS II mice treated with intraventricular ERT

An IDS was injected into the MPS II mice (16 week old) brain, which was repeated 6 times. Although alternation behavior in the disease-control, MPS II mouse group was significantly decreased compared with wild-type mice, this behavior was recovered in the IDS-treated MPS II mouse group (Table 1). MPS II mice exhibited an impairment in spontaneous alternation and behavior in a Y-maze compared with all other groups (one-way ANOVA *P ≤ 0.05). The arm entries in the MPS II control group were elevated, while the arm entries in the intraventricular ERT mice returned to normal levels.
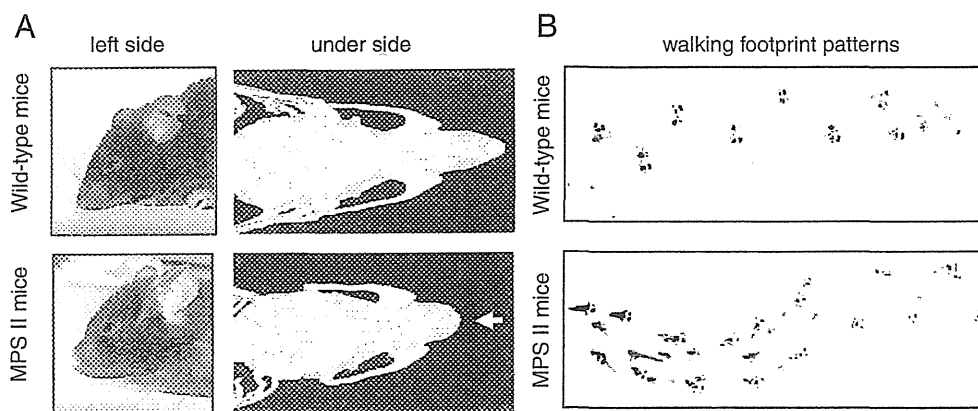
Fig. 1. The upper column shows the wild-type mouse, and the lower column shows the MPS II mouse. (A) Pictures show the left side of the face and an X-ray CT image of the head in a 21-week-old mouse. The arrow shows nose dysplasia in the MPS II mouse. (B) Walking footprint patterns show the forefoot (red) and hindfoot (black) in a 21-week-old mouse.
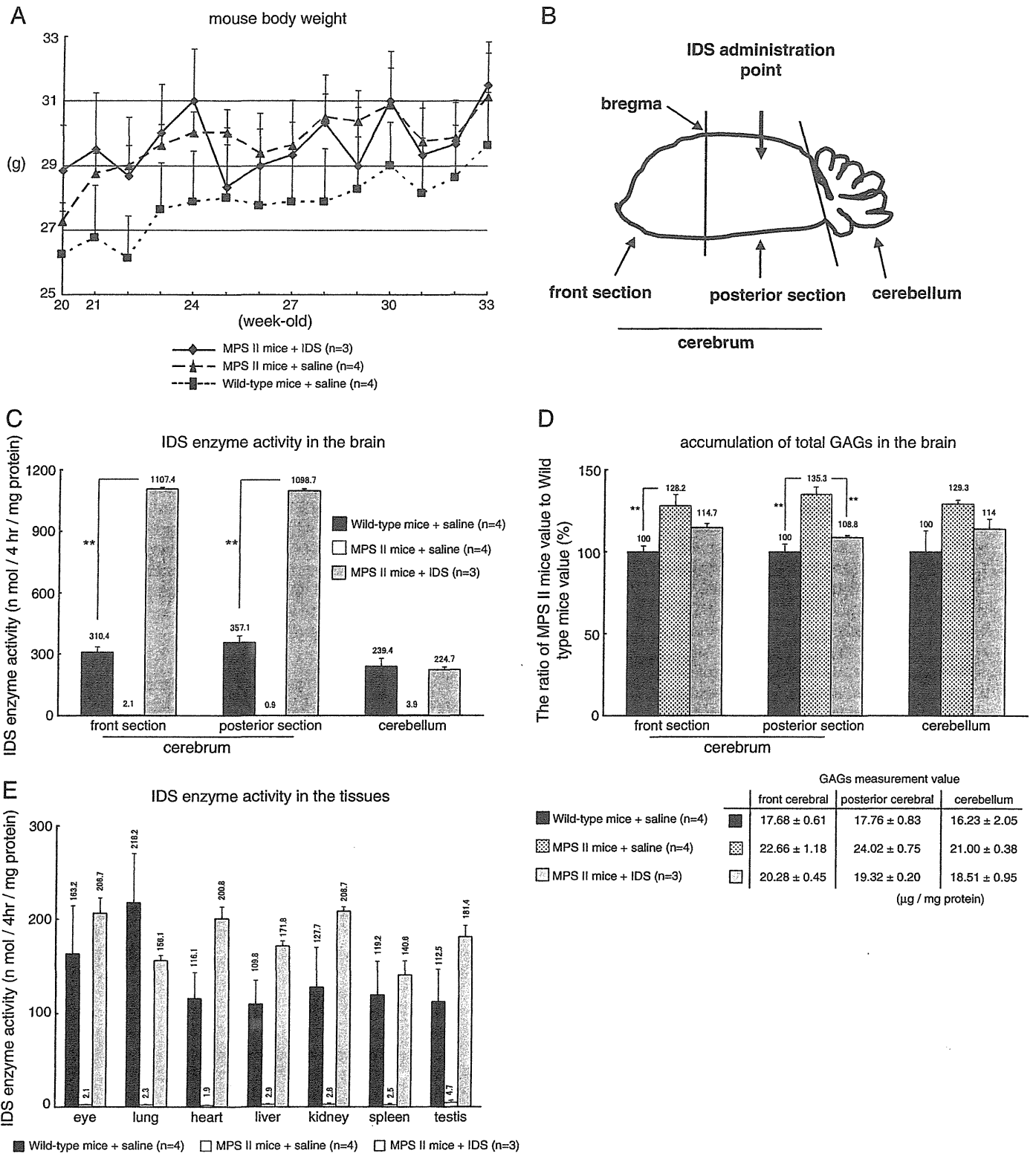
Fig. 2. (A) Average body weight change in MPS II mice treated with/without IDS. Error bars denote SEM. (B) Three brain regions of the cerebrum (front and posterior) and cerebellum. (C) Measurement of IDS enzyme activity in the brain treated with/without IDS using the MU-αIdu-2S enzyme activity assay. All the mice were sacrificed by transcardial perfusion with PBS. Error bars denote SEM. **: P<0.01 (D) measurement of total GAGs in the brain treated with/without IDS using Alucian blue-binding assay (control wild-type mice are 100%). The actual measurement value is shown in the figure. Error bars denote SEM. **: P<0.01 (E) measurement of IDS enzyme activity in the tissues treated with/without IDS using MU-αIdu-2S enzyme activity assay. All the mice were sacrificed by transcardial perfusion with PBS. Error bars denote the SEM.

3.3.2. Pathological analysis of the MPS II mouse treated with IDS administration via intraventricular ERT

Additional injections of the IDS were performed 2 times in the previous MPS II mouse (total 8 times). A pathologic analysis of the mouse brain, liver, and testis was performed (Fig. 3). In the MPS II mouse brain, many vacuolations were identified in the cytosol of the Purkinje cells and the margin cells of the cerebellum. These vacuoles were visualized with H&E and toluidine blue staining. Lamp2

Table 1
Analysis of alternation behavior and number of arm entries for 32-week-old MPS II mice using the Y-maze test. IDS intraventricular ERT protocol: IDS 20 μg/3 weeks × 6 times for a 16-week-old mouse. Each mouse was tested four times per experiment. Data were expressed as M ± SEM. One-way ANOVA *: P ≤ 0.05. N.S.: not significant.

| Effects of multiple IDS intraventricular ERT on Y-maze behavior		
	Alternation behavior (%)	Number of arm entries
Wild-type mice (n = 9)	69.53% ± 3.13	14.58 ± 1.294
MPS II mice + saline (n = 7)	59.55% ± 2.25	20.00 ± 1.783
MPS II mice + IDS (n = 3)	62.61% ± 6.90	13.42 ± 0.583

protein overexpression was observed in the cytosol of these cells. The liver cells also had many vacuoles, and Lamp2 was overexpressed throughout the entire liver. In the testis, many vacuoles were visualized, and Lamp2 protein was overexpressed in the Leydig cells. Following administration of IDS with intraventricular ERT, the number of vacuolations and the amount of Lamp2 protein were reduced in the brain, liver, and testis. The changes in the mouse face were also determined with/without administration of IDS via intraventricular ERT. The wild-type mice had a sharp nose, normal eyes, and good-quality hair, whereas the MPS II model mice had a coarse face and poor-quality hair. The MPS II mice treated with IDS had also a coarse face and poor-quality hair. However they were a little better than non-treated MPS II mice (data not shown).

4. Discussion

We used an iduronate-2-sulfatase-knockout, Hunter syndrome (mucopolysaccharidosis type II, MPS II) model mouse with a deletion in the *Ids* gene from exon 2 to exon 5. As a corollary, MPS II patients generally exhibit bone and joint disorders. In most cases, the face of the MPS II patient is coarse. X-ray analysis shows the characteristic features of MPS, such as marked skeletal hyperostosis and nose deformation [21]. The iduronate-2-sulfatase-knockout, MPS II model mouse has been reported to exhibit widespread bone deformities [14]. Our MPS II model mice had large round eyes, hyperostosis in the head and nose dysplasia (Fig. 1A). Furthermore, they walked with a short-stepped gait and a funny, waddling walk when compared with the wild-type mice (Fig. 1B). These results suggest that, similar to humans, their symptoms were caused by bone and joint dysfunctions. X-ray CT analysis and walking footprint analysis were appropriate methods for evaluating bone and joint diseases in the MPS II model mouse. The coarse face of the MPS II mice is similar to that of human MPS II patients. The cause of the nose dysostosis is total GAG accumulation in the bones.

The 21-week-old MPS II mice were injected with IDS into the lateral ventricle, which was performed 4 times over a period of 12 weeks. The body weights of mice treated with intraventricular ERT were measured (Fig. 2A). There was no significant difference in the weights in the intraventricular ERT group compared with those in the control group. We did not find any abnormal infiltration of inflammatory cells in the brain, liver, and spleen with pathological analysis (data not shown). In this experiment, mice that treated IDS had good coat and were fed normal chow. There was no significant change in body weight in mice. So we suspected that large stress of administration and serious immunological response against IDS had not occurred in the MPS II mouse. The IDS enzyme activity in the cerebrum of the IDS-treated group was significantly elevated compared with the disease-control mice (Fig. 2C). The enzyme activity in the front cerebral region was almost equal to that in the posterior cerebral region. It indicates that IDS was distributed through the entire
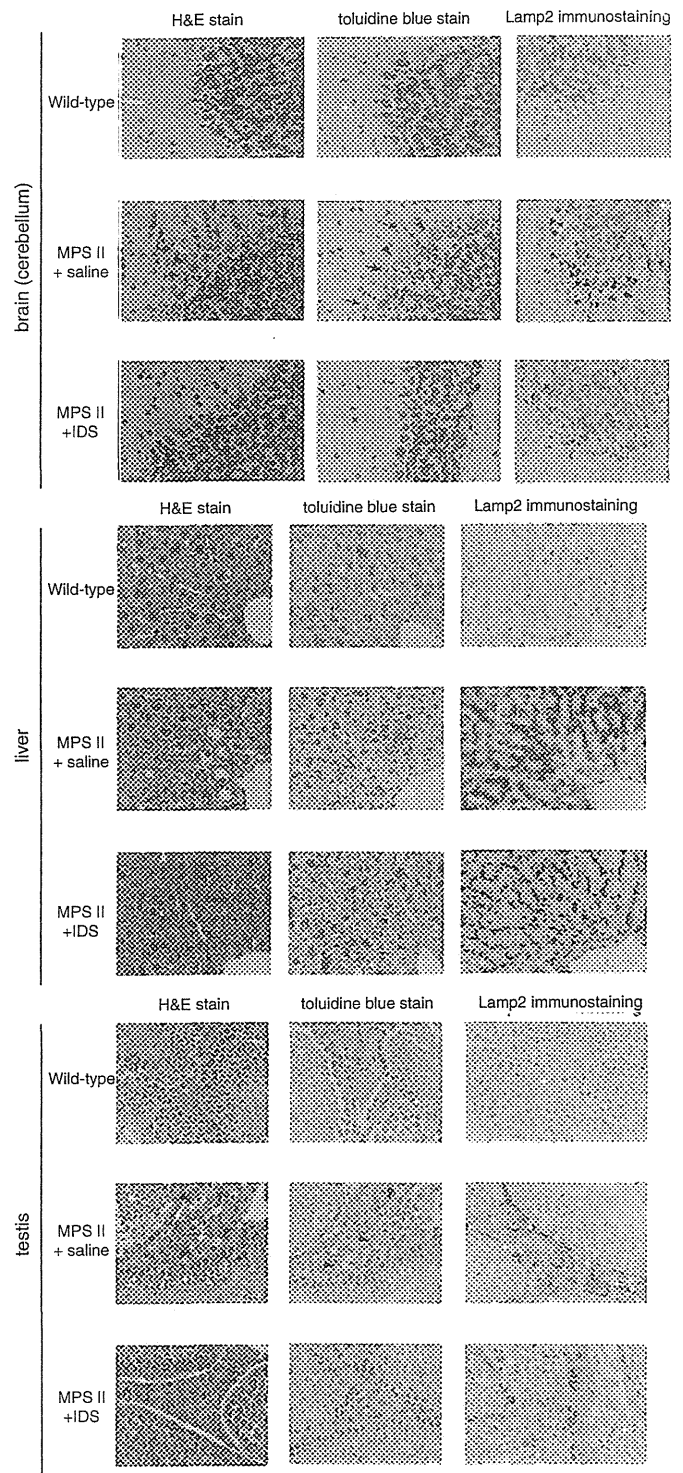
Fig. 3. H&E stain, toluidine blue stain and Lamp2 immunostaining analysis of 40-week-old mouse tissues treated with IDS via intraventricular ERT (brain (cerebellum), liver, and testis). Arrowhead design (▲) is a vacuole in the Purkinje cell, or Leydig cell. Arrow design (↑) is a vacuole in the margin cell of the Purkinje cell.

cerebrum via ventricular fluid. Although IDS enzyme activity in the cerebellum also increased, this level was equal to the level of IDS enzyme activity in the wild-type mouse. In the cerebellum, uptake of the IDS enzyme may be poor compared with uptake in the cerebrum. There might be some other mechanism about the poor uptake of IDS in the cerebellum. The contact area of IDS might be the difference between cerebrum and cerebellum. Or there might be a difference in the expression level of receptors (i.e. mannose-6-phosphate receptor)

between cerebrum and cerebellum. We measured the accumulation of total GAGs in three regions of the brain (Fig. 2D). Total GAGs in the disease-control MPS II group was elevated by 20–30% of the wild-type group. However, following treatment with IDS via 4 times intraventricular ERT, this accumulation was decreased by more than 50% of storage growth. In other tissues (eye, lung, heart, liver, kidney, spleen, and testis), IDS activity was increased to levels comparable to those in the wild-type mouse (Fig. 2E). The IDS injected into the lateral cerebral ventricle was distributed in the ventricular fluid. The fluid flows through to the spinal fluid. Thus, neuronal cells could directly uptake IDS instead of via BBB. We had expected an increase of IDS enzyme activity in brain-specific manner. However, contrary to expectations, the enzyme activity was also up in the tissues other than the brain. There is a report that showed a systemic effect of GDNF that was administered intracerebroventricular injections of GDNF [22]. So, there might be possibly some sort of drug transfer pathway from the brain to the body. The cerebrospinal fluid containing IDS might communicate with the systemic venous system via the subarachnoid space. So we hypothesize that the enzyme was carried via the bloodstream to many tissues.

We analyzed spontaneous alternation behavior in the MPS II mouse treated with multiple administrations of intraventricular ERT with the Y-maze test (Table 1). In many cases, MPS II patients have neurological involvement of their disease [23]. There are many previously published studies using MPS II murine models [24–27]. Until now, however, the study to analyze the MPS II mouse behaviors has not been done. Our study provides novel insight into MPS II mouse behavior and the effects of treatment with IDS via intraventricular ERT in the MPS II murine model. Alternation behavior (i.e., short-term working memory) was significantly decreased, and the number of arm entries (i.e., physical exertion or activity) was significantly increased in disease-control mice compared with wild-type mice. These data indicate that the MPS II model mouse may have short-term working memory dysfunction and overactivity. These data showed that administration of IDS via intraventricular ERT is an efficient method to improve brain functions in the MPS II mouse. The results of intraventricular enzyme administration in MPS II mice might be able to offer treatment methods for other mucopolysaccharidosis (MPS I) and also for many other LSD (Gaucher disease, Krabbe disease or metachromatic leukodystrophy) that exhibit neurologic symptoms [28–31].

The assessment of mice exposed to treatment with IDS via intraventricular ERT demonstrated that the appearance of the coarse face and hair was improved compared with untreated mice. Intraventricular ERT could treat neurological findings as well as systemic clinical features, such as hepatosplenomegaly, and skin, among others. There was no weight loss in the IDS-treated mouse, so we suspected that adverse events, such as an IDS-immunoreactive response, were not caused by IDS administration. Untreated MPS II mice exhibited a coarse face and looked older than treated mice. The round nose did not improve in the treated mice. After 16-weeks of age mice were less responsive to ERT for bone involvement. Moreover, we analyzed many mouse tissues with histological procedures, such as hematoxilin-eosin staining, toluidine blue staining and Lamp2 immunostaining (Fig. 3). Although the cerebrum of MPS II mice exhibited changes compared with wild-type and treated mice, there was a significant pathological difference in the cerebellum. There were massive vacuolations in the cell body of Purkinje cells and in the margin cells. Additionally, the Lamp2 protein, a lysosome marker, was also overexpressed in those cells. The cerebellum might have more pathological involvement than the cerebrum. Hepatomegaly is one major symptom in MPS II patients [32]. There were large and massive vacuoles, and overexpression of the Lamp2 protein, in a widespread area of the liver in the disease control mouse. The liver had a tendency to become heavier when compared with wild-type and IDS-treated mice (data not shown). Our iduronate-2-sulfatase-deficient, MPS II model mouse displays an increased incidence of male infertility. The HOS (Hunter Outcome Survey) study also indicated that a higher incidence of infertility has been reported in MPS II patients [33]. The genitourinary complications in MPS II have been noted because the testis also shows pathological involvement. The testis contained massive vacuoles and stained heavily with Lamp2, especially in the tubular epithelial cells and the Leydig cells. Although histological findings in the brain, liver and testis cells were significantly improved by treatment with IDS via intraventricular ERT. It is intriguing that intraventricular administration of the IDS enzyme clearly stimulated enzyme activity in the CNS cells in addition to the various systemic tissues, such as the liver, spleen, testis and kidney cells. Therefore, intraventricular ERT can treat neurological findings as well as systemic clinical features, such as hepatosplenomegaly, skin, and among others.

5. Conclusions

The recombinant human iduronate-2-sulfatase administration via intraventricular ERT led to stimulation of the enzyme in the brain in addition to other tissues (liver, spleen, testis, etc.) in the mouse. Furthermore, administration of the IDS via intraventricular ERT improved brain functions including short-term memory and behavior. These results demonstrate the possible efficacy of an ERT procedure with intraventricular administration of IDS for the treatment of MPS II.

Acknowledgments

References

[1] M. Scarpa, Z. Almássy, M. Beck, O. Bodamer, I.A. Bruce, L. De Meirleir, N. Guffon, E. Guillén-Navarro, P. Hensman, S. Jones, W. Kamin, C. Kampmann, C. Lampe, C.A. Lavery, E. Leão Teles, B. Link, A.M. Lund, G. Malm, S. Pitz, M. Rothera, C. Stewart, A. Tylki-Szymańska, A. van der Ploeg, R. Walker, J. Zeman, J.E. Wraith, Mucopolysaccharidosis type II: European recommendations for the diagnosis and multidisciplinary management of a rare disease, Orphanet J. Rare Dis. 6 (2011) 72.
[2] T. Okuyama, A. Tanaka, Y. Suzuki, H. Ida, T. Tanaka, G.F. Cox, Y. Eto, T. Orii, Japan Elaprase Treatment (JET) study: idursulfase enzyme replacement therapy in adult patients with attenuated Hunter syndrome (Mucopolysaccharidosis II, MPS II), Mol. Genet. Metab. 99 (2010) 18–25.
[3] F. Papadia, M.S. Lozupone, A. Gaeta, D. Capodiferro, G. Lacalendola, Long-term enzyme replacement therapy in a severe case of mucopolysaccharidosis type II (Hunter syndrome), Eur. Rev. Med. Pharmacol. Sci. 15 (2011) 253–258.
[4] J. Donaldson, W.S. Khan, H. Tailor, D.A. Hughes, A.M. Mehta, N. Maruthainar, Gaucher disease: outcome following total hip replacements and effect of enzyme replacement therapy in a cohort of UK patients, Hip Int. 21 (2011) 665–671.
[5] C. Angelini, C. Semplicini, Enzyme replacement therapy for Pompe disease, Curr. Neurol. Neurosci. Rep. 12 (2012) 70–75.
[6] R.C. Desnick, M. Banikazemi, Fabry disease: clinical spectrum and evidence-based enzyme replacement therapy, Nephrol. Ther. 2 (2006) 172–185.
[7] K.M. Newkirk, R.M. Atkins, P.I. Dickson, B.W. Rohrbach, M.F. McEntee, Ocular lesions in canine mucopolysaccharidosis I and response to enzyme replacement therapy, Invest. Ophthalmol. Vis. Sci. 11 (2011) 5130–5135.
[8] E. Glamuzina, E. Fettes, K. Bainbridge, V. Crook, N. Finnegan, L. Abulhoul, A. Vellodi, Treatment of mucopolysaccharidosis type II (Hunter syndrome) with idursulfase: the relevance of clinical trial end points, J. Inherit. Metab. Dis. 34 (2011) 749–754.
[9] V. Valayannopoulos, H. Nicely, P. Harmatz, S. Turbeville, Mucopolysaccharidosis VI, Orphanet J. Rare Dis. 12 (2010) 5.
[10] S. Al Sawaf, E. Mayatepek, B. Hoffmann, Neurological findings in Hunter disease: pathology and possible therapeutic effects reviewed, J. Inherit. Metab. Dis. 31 (2008) 473–480.

[11] Q. Zhou, R.J. Boado, J.Z. Lu, E.K. Hui, W.M. Pardridge, Brain-penetrating IgG-iduronate 2-sulfatase fusion protein for the mouse, Drug Metab. Dispos. 40 (2012) 329–335.

[12] D. Tsuji, H. Akeboshi, K. Matsuoka, H. Yasuoka, E. Miyasaki, Y. Kasahara, I. Kawashima, Y. Chiba, Y. Jigami, T. Taki, H. Sakuraba, K. Itoh, Highly phosphomannosylated enzyme replacement therapy for GM2 gangliosidosis, Ann. Neurol. 69 (2011) 691–701.

[13] P. Dickson, M. McEntee, C. Vogler, S. Le, B. Levy, M. Peinovich, S. Hanson, M. Passage, E. Kakkis, Intrathecal enzyme replacement therapy: successful treatment of brain disease via the cerebrospinal fluid, Mol. Genet. Metab. 91 (2007) 61–68.

[14] M. Cardone, V.A. Polito, S. Pepe, L. Mann, A. D'Azzo, A. Auricchio, A. Ballabio, M.P. Cosma, Correction of Hunter syndrome in the MPSII mouse model by AAV2/8-mediated gene delivery, Hum. Mol. Genet. 1 (2006) 1225–1236.

[15] A.R. Garcia, J.M. DaCosta, J. Pan, J. Muenzer, J.C. Lamsa, Preclinical dose ranging studies for enzyme replacement therapy with idursulfase in a knock-out mouse model of MPS II, Mol. Genet. Metab. 91 (2007) 183–190.

[16] K. Schmaltz, R.J. Katz, Y-maze behavior in the mouse after morphine or an enkephalin analog, Psychopharmacology (Berl) 74 (1981) 99–100.

[17] K. Washida, M. Ihara, K. Nishio, Y. Fujita, T. Maki, M. Yamada, J. Takahashi, X. Wu, T. Kihara, H. Ito, H. Tomimoto, R. Takahashi, Nonhypotensive dose of telmisartan attenuates cognitive impairment partially due to peroxisome proliferator-activated receptor-gamma activation in mice with chronic cerebral hypoperfusion, Stroke 41 (2010) 1798–1806.

[18] S. Kawagoe, T. Higuchi, X.L. Meng, Y. Shimada, H. Shimizu, R. Hirayama, T. Fukuda, H. Chang, T. Nakahata, S. Fukada, H. Ida, H. Kobayashi, T. Ohashi, Y. Eto, Generation of induced pluripotent stem (iPS) cells derived from a murine model of Pompe disease and differentiation of Pompe-iPS cells into skeletal muscle cells, Mol. Genet. Metab. 104 (2011) 123–128.

[19] Y. Shimada, H. Nishida, Y. Nishiyama, H. Kobayashi, T. Higuchi, Y. Eto, H. Ida, T. Ohashi, Proteasome inhibitors improve the function of mutant lysosomal α-glucosidase in fibroblasts from Pompe disease patient carrying c.546G>T mutation, Biochem. Biophys. Res. Commun. 18 (2011) 274–278.

[20] T. Fukuda, N. Akiyama, M. Ikegami, H. Takahashi, A. Sasaki, H. Oka, T. Komori, Y. Tanaka, Y. Nakazato, J. Akimoto, J. Tanaka, Y. Okada, S. Saito, Expression of hydroxyindole-O-methyltransferase enzyme in the human central nervous system and in pineal parenchymal cell tumors, J. Neuropathol. Exp. Neurol. 69 (2010) 498–510.

[21] T. Demitsu, M. Kakurai, Y. Okubo, C. Shibayama, Y. Kikuchi, Y. Mori, K. Sukegawa, M. Mizuguchi, Skin eruption as the presenting sign of Hunter syndrome IIB, Clin. Exp. Dermatol. 24 (1999) 179–182.

[22] J.H. Kordower, S. Palfi, E.Y. Chen, S.Y. Ma, T. Sendera, E.J. Cochran, E.J. Mufson, R. Penn, C.G. Goetz, C.D. Comella, Clinicopathological findings following intraventricular glial-derived neurotrophic factor treatment in a patient with Parkinson's disease, Ann. Neurol. 46 (1999) 419–424.

[23] B. Link, L.L. de Camargo Pinto, R. Giugliani, J.E. Wraith, N. Guffon, E. Eich, M. Beck, Orthopedic manifestations in patients with mucopolysaccharidosis type II (Hunter syndrome) enrolled in the Hunter Outcome Survey, Orthop. Rev. (Pavia) 23 (2010) 56–64.

[24] A.R. Garcia, J. Pan, J.C. Lamsa, J. Muenzer, The characterization of a murine model of mucopolysaccharidosis II (Hunter syndrome), J. Inherit. Metab. Dis. 30 (2007) 924–934.

[25] V.A. Polito, M.P. Cosma, IDS crossing of the blood–brain barrier corrects CNS defects in MPSII mice, Am. J. Hum. Genet. 85 (2009) 296–301.

[26] S.C. Jung, E.S. Park, E.N. Choi, C.H. Kim, S.J. Kim, D.K. Jin, Characterization of a novel mucopolysaccharidosis type II mouse model and recombinant AAV2/8 vector-mediated gene therapy, Mol. Cells 30 (2010) 13–18.

[27] V.A. Polito, S. Abbondante, R.S. Polishchuk, E. Nusco, R. Salvia, M.P. Cosma, Correction of CNS defects in the MPSII mouse model via systemic enzyme replacement therapy, Hum. Mol. Genet. 15 (2010) 4871–4885.

[28] R.Y. Wang, E.J. Cambray-Forker, K. Ohanian, D.S. Karlin, K.K. Covault, P.H. Schwartz, J.E. Abdenur, Treatment reduces or stabilizes brain imaging abnormalities in patients with MPS I and II, Mol. Genet. Metab. 98 (2009) 406–411.

[29] C. Mignot, Clinical aspects of early-stage neurological forms of Gaucher disease, Rev. Med. Interne 1 (2006) 14–17.

[30] G.M. Pastores, Krabbe disease: an overview, Int. J. Clin. Pharmacol. Ther. 47 (2009) 75–81.

[31] V. Gieselmann, I. Krägeloh-Mann, Metachromatic leukodystrophy—an update, Neuropediatrics 41 (2010) 1–6.

[32] C.P. Chen, S.P. Lin, C.Y. Tzen, W.L. Hwu, S.R. Chern, C.K. Chuang, S.S. Chiang, W. Wang, Prenatal diagnosis and genetic counseling of mucopolysaccharidosis type II (Hunter syndrome), Genet. Couns. 18 (2007) 49–56.

[33] J.E. Wraith, M. Beck, R. Giugliani, J. Clarke, R. Martin, J. Muenzer, HOS Investigators, Initial report from the Hunter Outcome Survey, Genet. Med. 10 (2008) 508–516.
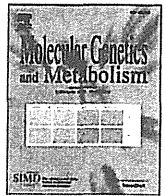
Akt inactivation induces endoplasmic reticulum stress-independent autophagy in fibroblasts from patients with Pompe disease

Yurika Nishiyama [a,b], Yohta Shimada [a,*], Takayuki Yokoi [a,b], Hiroshi Kobayashi [a,b,c], Takashi Higuchi [c], Yoshikatsu Eto [c], Hiroyuki Ida [a,b,c], Toya Ohashi [a,b,c]

[a] Department of Gene Therapy, Institute of DNA Medicine, The Jikei University School of Medicine, Tokyo 105-8461, Japan
[b] Department of Pediatrics, The Jikei University School of Medicine, Tokyo 105-8461, Japan
[c] Department of Genetic Diseases & Genomic Science, The Jikei University School of Medicine, Tokyo 105-8461, Japan

ARTICLE INFO

ABSTRACT

Pompe disease (glycogen storage disease type II) is an autosomal recessive neuromuscular disorder arising from a deficiency of lysosomal acid α-glucosidase (GAA). Accumulation of autophagosomes is a key pathological change in skeletal muscle fibers and fibroblasts from patients with Pompe disease and is implicated in the poor response to enzyme replacement therapy (ERT). We previously found that mutant GAA-induced endoplasmic reticulum (ER) stress initiated autophagy in patient fibroblasts. However, the mechanism of induction of autophagy in fibroblasts from Pompe disease patients lacking ER stress remains unclear. In this study, we show that inactivated Akt induces ER stress-independent autophagy via mTOR suppression in patient fibroblasts. Activated autophagy as evidenced by increased levels of LC3-II and autophagic vesicles was observed in patient fibroblasts, whereas PERK phosphorylation reflecting the presence of ER stress was not observed in them. These patient fibroblasts showed decreased levels of not only phosphorylated Akt, but also phosphorylated p70 S6 kinase. Treatment with insulin, which acts as an activator of the Akt signaling pathway, resulted in increased phosphorylation of both Akt and p70 S6 kinase and suppression of autophagy in patient fibroblasts. In addition, following combination treatment with recombinant human GAA plus insulin, enhanced localization of the enzymes with lysosomes was observed in patient fibroblasts. These findings define a critical role of Akt suppression in the induction of autophagy in fibroblasts from patients with Pompe disease carrying an ER stress non-inducible mutation, and they provide evidence that insulin may potentiate the effect of ERT.

© 2012 Elsevier Inc. All rights reserved.

1. Introduction

Pompe disease (glycogen-storage disease type II) is an autosomal recessive lysosomal storage disorder caused by a deficiency of acid α-glucosidase (GAA) which leads to progressive intralysosomal accumulation of glycogen [1]. The lack of GAA activity results in cellular dysfunction in multiple tissues, particularly cardiac and skeletal muscles. Infantile-onset forms of the disease present progressive generalized muscle weakness and hypertrophic cardiomyopathy with death occurring within the first few months of life from cardiorespiratory failure [2]. Milder late-onset forms are characterized by a slowly progressing skeletal myopathy without severe cardiac symptoms [3].

Enzyme replacement therapy (ERT) with recombinant human GAA (rhGAA) is now available for treating Pompe disease. ERT has been shown to alleviate the cardiac symptoms and prolong the lifespan of patients with the infantile form of the disease [4], but its effect on skeletal muscle pathology is very limited. This lack of efficacy is, in part, due to the accumulation of autophagic vesicles, which has been observed in skeletal muscle fibers from patients and mouse models of Pompe disease in the same manner as glycogen-filled lysosomes [5,6]. In GAA knock-out mice, accumulated autophagic vacuoles have been shown to trap endocytosed rhGAA and interfere with trafficking of the recombinant enzyme to lysosomes in type II skeletal muscle fibers [5].

Macroautophagy (referred to hereafter as autophagy) is a constitutive lysosomal degradation process that is required to supply nutrients under starvation conditions and to maintain cellular homeostasis through the elimination of abnormal proteins and damaged organelles [7]. During autophagy, cellular components are engulfed by the double-membrane autophagosome, which fuses with lysosomes to degrade the internal contents. We and others have previously reported that autophagosomes accumulate in fibroblasts from patients with Pompe disease [8,9]. We also demonstrated that mutant GAA-induced endoplasmic reticulum (ER) stress is involved in the induction of autophagy in fibroblasts from patients [8]. However, autophagic buildup is observed in GAA knock-out mice despite the complete lack of GAA protein [10], indicating another trigger, aside from ER stress, for autophagy induction in GAA deficiency.

In the present study, we show that protein kinase B (Akt) is inactivated and regulates autophagy through the mTOR pathway in fibroblasts lacking ER stress. In addition, we demonstrate that treatment with insulin enhances delivery of rhGAA to lysosomes in fibroblasts from patients with Pompe disease.

2. Materials and methods

2.1. Chemicals and antibodies

Protease inhibitor cocktail (PIC) was purchased from Roche Diagnostics (Indianapolis, IN). Tunicamycin and Akt inhibitor VIII were obtained from Calbiochem (La Jolla, CA). Anti-GAA antibody and rhGAA were gifts from Genzyme Corporation (Cambridge, MA). Anti-phosphorylated PERK antibody and anti-LAMP2 antibody were obtained from Santa Cruz Biotechnology (Santa Cruz, CA). Anti-LC3 antibody was obtained from Novus Biologicals (Litteleton, CO). Anti-phosphorylated Akt antibody and anti-phosphorylated p70 S6 kinase antibody were purchased from Cell Signaling Technology (Beverly, MA). Anti-actin antibody, insulin and all other chemicals were obtained from Sigma (St. Louis, MO).

2.2. Fibroblast cultures

Skin fibroblasts from patients with infantile-onset Pompe disease (GM00248: P1 fibroblasts; GM20090: P2 fibroblasts; Coriell Institute for Medical Research, Camden, NJ) and a healthy individual (NB1RGB; Riken Bioresource Center, Ibaraki, Japan) were maintained at subconfluent densities in Dulbecco's modified Eagle's medium (DMEM) supplemented with 25 mM glucose and 10% fetal bovine serum at 37 °C (with 5% CO_2). For a low glucose treatment, the fibroblasts were cultured in DMEM supplemented with 5.5 mM glucose and 10% fetal bovine serum at 37 °C (with 5% CO_2).

2.3. Preparation of cell extracts for Western blot analysis

Protein samples for Western blot analysis were prepared as previously described [11]. Briefly, fibroblasts were washed three times with ice-cold phosphate-buffered saline (PBS) and lyzed with lysis buffer (50 mM Tris–HCl, pH 7.5 containing 2% SDS and PIC). Samples were centrifuged for 1 h at 18,000 ×g at 4 °C. The supernatants were used as whole-cell lysates. Protein concentrations were estimated by using the DC protein assay (Bio-Rad, Hercules, CA) standardized with bovine
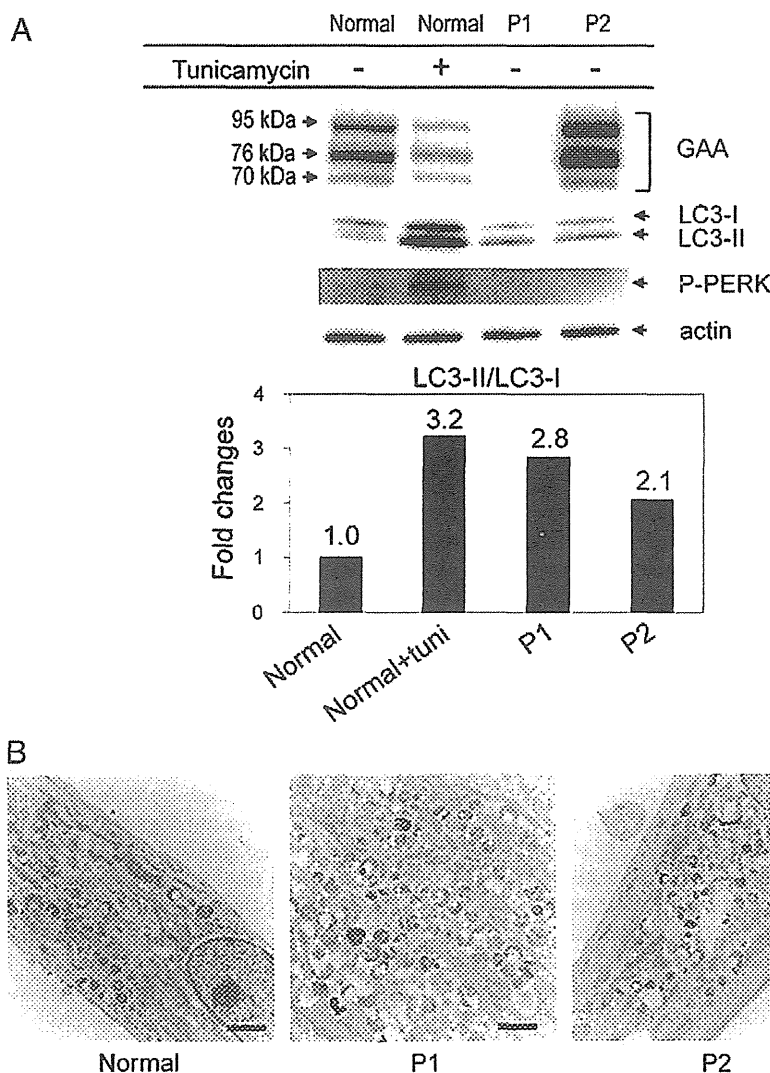
Fig. 1. Autophagy in patient fibroblasts carrying an ER stress-non inducible mutation. (A) Western blot analysis of GAA, phosphorylated PERK, and LC3 in patient fibroblasts. Normal fibroblasts were cultured for 24 h in the presence (+) or absence (−) of 2 μg/ml tunicamycin, an ER stress inducer (Normal + tuni). Patient fibroblasts (P1 and P2) and normal fibroblasts were solubilized with lysis buffer. The samples were resolved by SDS-PAGE, blotted, and probed with antibodies against GAA, phosphorylated PERK (P-PERK), LC3, and actin. The level of actin was analyzed as the internal control. The band intensities of LC3-II were quantified by densitometry and normalized to LC3-I. Densitometric values in the histograms are expressed as fold-change relative to the normal, which was assigned a value of 1. (B) Electron micrographs of patient fibroblasts (P1 and P2). Autophagic vesicles were seen in the cytoplasm of patient fibroblasts. Scale bar, 2 μm.

serum albumin. Equal amounts of proteins were resolved by SDS-PAGE on 4–20% acrylamide gradient gels and transferred onto a nitrocellulose membrane. The membranes were blocked with a blocking buffer (50 mM Tris–HCl, pH 7.5 containing 150 mM NaCl, 0.1% gelatin, 0.1% casein, and 0.05% Tween 20) and then incubated with each primary antibody. After a brief washing, the membranes were incubated with peroxidase-labeled secondary antibody (Nichirei Corp., Tokyo, Japan) and visualized by using Immunostar LD (Wako Pure Chemicals, Tokyo, Japan).

2.4. Immunocytochemistry

Fluorescence immunostaining against both rhGAA and LAMP2 was performed according to a previously described procedure [11]. Briefly, normal and patient fibroblasts grown on coverslips were fixed with 4% paraformaldehyde, and permeabilized by using PBS containing 0.1% Triton X-100, and blocked with PBS containing 10% normal goat serum (Vector Laboratories, Burlingame, CA). These cells were incubated with the primary antibody and visualized by incubation with Alexa 488- or 594-conjugated secondary antibodies (Invitrogen, Carlsbad, CA). These fibroblasts were counterstained with DAPI (Vector Laboratories), mounted, and observed with an inverted Olympus IX-70 microscope equipped with epifluorescence.

2.5. Electron microscopy

Electron microscopy analysis was performed as previously described [8]. Briefly, normal and patient fibroblasts were double-fixed with 2% glutaraldehyde/0.1 M phosphate buffer (PB) and 1% osmium tetroxide/0.1 M PB. These fibroblasts were dehydrated with an ethanol gradient, and embedded in epoxy resin. Ultrathin sections were stained with uranyl acetate and lead citrate, and observed with a Hitachi H7500 electron microscope (Hitachi, Tokyo, Japan).

3. Results

3.1. ER stress-independent autophagy in fibroblasts from patients with Pompe disease

To determine whether autophagy is induced in fibroblasts from patients with Pompe disease, whole-cell lysates prepared from normal and patient fibroblasts (P1 and P2) were analyzed by Western blotting with anti-LC3 antibody. The levels of LC3-II, a major constituent of autophagosomes, were higher in both patient fibroblasts (P1 and P2) than in normal fibroblasts (Fig. 1A). Moreover, to morphologically evaluate autophagy in patient fibroblasts, we analyzed both patient and normal fibroblasts by using electron microscopy. Ultrastructural analysis revealed the accumulation of autophagic vesicles containing multilamellar structures in patient fibroblasts (Fig. 1B), indicating that autophagy is increased in both P1 and P2 fibroblasts.

Because we have previously demonstrated that mutant GAA-induced ER stress is involved in the induction of autophagy in fibroblasts from patients with late-onset Pompe disease [8], we next analyzed the levels of GAA and phosphorylated PERK in P1 and P2 fibroblasts by using Western blotting. Almost no GAA bands were detected in P1 fibroblasts, but bands corresponding to 70 kDa minor mature, 76 kDa major mature, and 95 kDa intermediate forms were observed in P2 fibroblasts (Fig. 1A). In addition, whereas phosphorylation of PERK (ER stress sensor) was observed in the normal fibroblasts exposed to tunicamycin (an ER stress inducer), it was not detected among normal fibroblasts that had not been exposed to the ER stress inducer or among patient fibroblasts (Fig. 1A). These results indicate that the induction of autophagy in P1 and P2 fibroblasts is triggered in an ER stress-independent manner.

3.2. Inactivation of Akt mediates induction of ER stress-independent autophagy in fibroblasts from patients with Pompe disease

The Akt signaling pathway is known to negatively regulate autophagy through phosphorylation of mTOR in addition to positively regulating glycogen synthesis [12,13]. To explore the contribution of the Akt/mTOR pathway to autophagy in P1 and P2 fibroblasts, we analyzed levels of phosphorylated Akt and phosphorylated p70 S6 kinase in patient fibroblasts. Phosphorylated Akt was almost absent in patient fibroblasts, in contrast to the normal fibroblasts in which Akt phosphorylation was clearly detected (lane LG − in Fig. 2). Additionally, decreased levels of phosphorylated p70 S6 kinase, which reflects mTOR activity [14], were observed in patient fibroblasts (lane LG − in Fig. 2), suggesting that suppression of the Akt/mTOR pathway contributes to the induction of autophagy in patient fibroblasts.

Next, to confirm the role of Akt in autophagy induction in patient fibroblasts, we examined the effect of modulation of Akt activity. Because phosphorylated Akt in cultured cells is known to be decreased by low glucose levels [15,16], we cultivated normal and patient fibroblasts in media containing low glucose and analyzed the levels of phosphorylated Akt, phosphorylated p70 S6 kinase, and LC3. Although low glucose decreased the levels of both phosphorylated Akt and phosphorylated p70 S6 kinase while increasing the levels of LC3-II in normal fibroblasts, no significant changes were observed in patient fibroblasts (Fig. 2).

In contrast, when patient fibroblasts were treated with insulin, which is an activator of the Akt pathway, increased phosphorylation of both Akt and p70 S6 kinase and attenuated conversion of LC3-I to LC3-II were observed in patient fibroblasts (Fig. 3A). The inhibitory effect of insulin on autophagy in patient fibroblasts was also confirmed by electron microscopy (Fig. 3B). Moreover, both increased levels of phosphorylated p70 S6 kinase and decreased conversion of LC3 in insulin-treated patient fibroblasts were abolished by treatment with Akt inhibitor VIII (Fig. 3C). These results suggest that inactivated Akt induces autophagy through suppression of mTOR activity in fibroblasts from patients with Pompe disease.
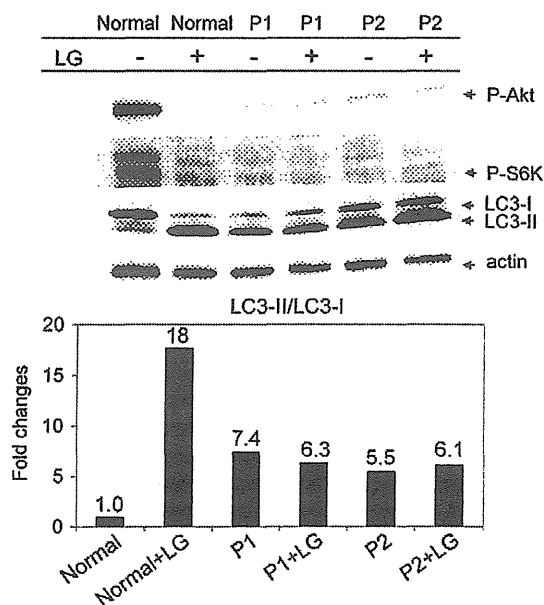
Fig. 2. Akt/mTOR pathway-related proteins in patient fibroblasts. Normal and patient fibroblasts (P1 and P2) were cultured in DMEM supplemented with 25 mM (LG −) or 5.5 mM glucose (LG +). Whole-cell extracts were electrophoresed followed by immunoblotting by using antibodies against phosphorylated Akt (P-Akt), phosphorylated p70 S6 kinase (P-S6K), LC3, and actin. The band intensities of LC3-II were quantified by densitometry and normalized to LC3-I. Densitometric values in the histograms are expressed as fold-change relative to the value in normal fibroblasts, which was assigned a value of 1.

493
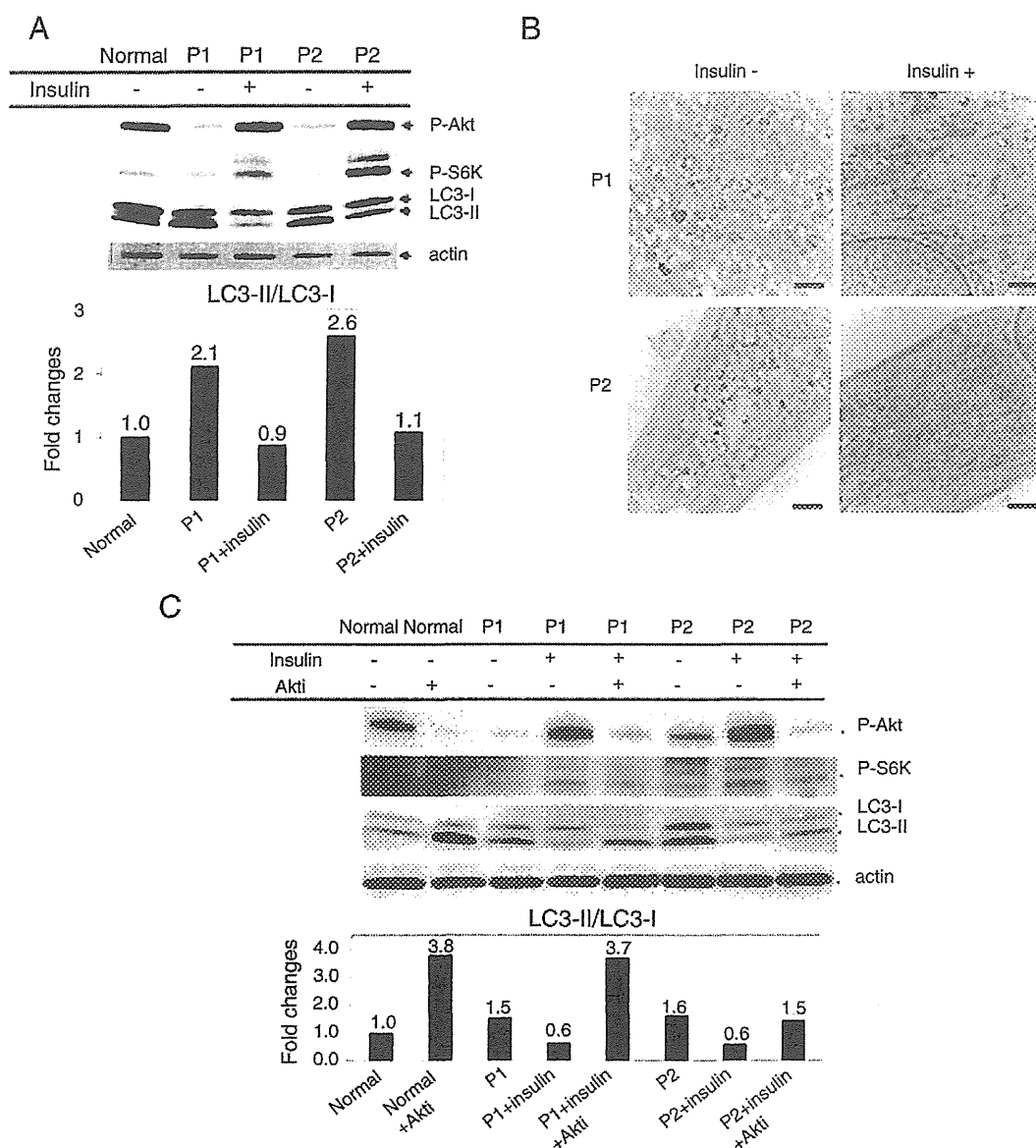
Fig. 3. Insulin inhibits the induction of autophagy through stimulation of Akt in patient fibroblasts. (A) Effects of insulin on levels of phosphorylated Akt, phosphorylated p70 S6 kinase, and LC3 in patient fibroblasts. Patient fibroblasts (P1 and P2) were cultured for 4 h in the presence (+) or absence (−) of 100 nM insulin. Whole-cell lysates from patient and normal fibroblasts were electrophoresed and blotted with anti-phosphorylated Akt antibody (P-Akt), anti-phosphorylated p70 S6 kinase antibody (P-S6K), anti-LC3 antibody, and anti-actin antibody. The band intensities of LC3-II were quantified by densitometry and normalized to LC3-I. Densitometric values in the histograms are expressed as fold-change relative to the value in normal fibroblasts, which was assigned a value of 1. (B) Electron micrographs of insulin-treated patient fibroblasts (P1 and P2). No accumulation of autophagic vacuoles is evident in the fibroblast cytoplasm. Scale bar, 2 μm. (C) Effect of Akt inhibitor on levels of phosphorylated Akt, phosphorylated p70 S6 kinase and LC3 in insulin-treated patient fibroblasts. Patient fibroblasts (P1 and P2) were pretreated with 100 nM insulin (3 h) and further cultured for 1 h in the presence (+) or absence (−) of 1 μM Akt inhibitor VIII (Akti). Whole-cell lysates from patient and normal fibroblasts were electrophoresed and blotted, and probed with antibodies against P-Akt, P-S6K, LC3, and actin. The band intensities of LC3-II were quantified by densitometry and normalized to LC3-I. Densitometric values in the histograms are expressed as fold-change relative to the value in normal fibroblasts, which was assigned a value of 1.

3.3. Activation of Akt improves the subcellular localization of rhGAA in fibroblasts from patients with Pompe disease

Accumulation of autophagic vacuoles has been shown to interfere with localization of rhGAA to lysosomes in skeletal muscles from GAA knock-out mice [5]. To investigate whether the activation of the Akt pathway positively affects trafficking of rhGAA, we incubated P1 fibroblasts, which have no endogenous GAA and show greater responsiveness to insulin than P2 fibroblasts (Figs. 1A and 3), with rhGAA after treatment with insulin, and analyzed the levels of recombinant enzymes in them. In P1 fibroblasts, treatment with a combination of rhGAA and insulin resulted in an increased ratio of 76 kDa mature forms to 110 kDa precursor forms, compared to treatment with the recombinant enzyme alone (Fig. 4A). Additionally, treatment with

insulin increased colocalization of rhGAA with LAMP2 in patient fibroblasts (Fig. 4B). These findings indicate that activation of Akt enhances the delivery of rhGAA to lysosomes in fibroblasts from patients with Pompe disease.

4. Discussion

In this study, we demonstrated the presence of both induction of autophagy and suppression of Akt in fibroblasts from patients with Pompe disease, in the absence of activation of ER stress (Figs. 1 and 2). Additionally, we have shown that activated Akt not only suppresses autophagy, but also improves subcellular trafficking of rhGAA in patient fibroblasts (Figs. 3 and 4). Our findings indicate the contribution of abnormal Akt signaling to ER stress-independent autophagy in fibroblasts

A

B
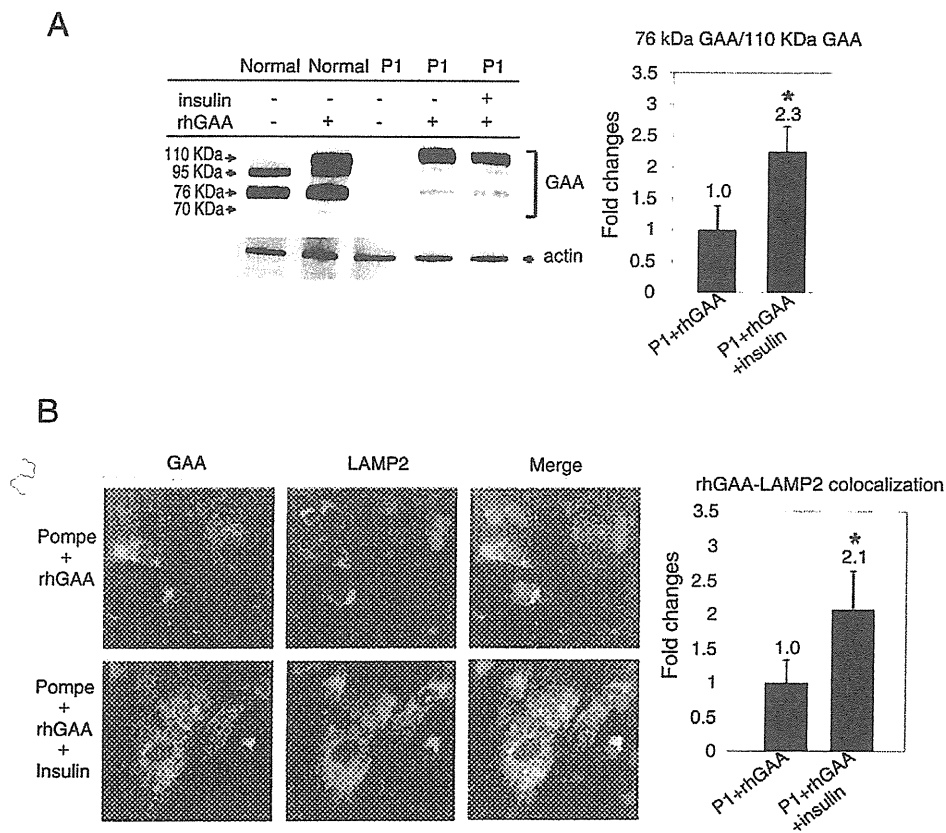
Fig. 4. Insulin enhances the subcellular localization of rhGAA with lysosomes in patient fibroblasts. (A) Effect of insulin on levels of GAA maturation in rhGAA-treated patient fibroblasts. P1 and normal fibroblasts were incubated with (+) or without (−) 100 nM insulin (4 h) and further treated with (+) or without (−) 10 μg/ml rhGAA (48 h). Whole-cell lysates were electrophoresed and blotted with anti-GAA antibody, and anti-actin antibody. The band intensities of 76 kDa GAA were quantified by densitometry and normalized to 110 kDa GAA. Densitometric values in the histograms are expressed as fold-change relative to the value in rhGAA-treated P1 fibroblasts, which was assigned a value of 1. Data are expressed as mean±SD (n=3) and statistical analysis was performed by use of Student's t test. * p<0.05. (B) Immunocytochemical analysis of rhGAA and LAMP2 in insulin-treated patient fibroblasts. P1 fibroblasts (Pompe) were incubated with (+) or without (−) 100 nM insulin (4 h) and further treated with 10 μg/ml rhGAA (48 h). The cells were fixed and stained with anti-GAA antibody and anti-LAMP2 antibody. The nuclei were counterstained with DAPI. The rate of rhGAA colocalizing with LAMP2 was evaluated. Fluorometric values in the histograms are expressed as fold-change relative to the value in rhGAA-treated P1 fibroblasts, which was assigned a value of 1. Data are expressed as mean±SD (n=5) and statistical analysis was performed by use of Student's t test. * p<0.05.

from patients with Pompe disease. Induction of autophagy is also observed in GAA-deficient mice which completely lack GAA mRNA and protein [10]. In addition, it has been reported that GSK-3β, which is inhibited by phosphorylated Akt, is activated in skeletal muscles from GAA knock-out mice [17]. It appears, therefore, that dysregulation of Akt signaling is a common trigger of autophagy in cells from Pompe disease patients and GAA-deficient mice. Akt is a widely expressed serine/threonine protein kinase that plays a central role in the regulation of cell survival, proliferation, and cellular metabolism [12]. In particular, this kinase is known to positively regulate glycogen synthase through phosphorylation of GSK3 [18]. In addition to its role in glycogen metabolism, Akt has been shown to be involved in the regulation of autophagy [13] and to inhibit autophagy through mTOR-dependent and -independent mechanisms in many cell types [19–21].

Because GAA catalyzes the lysosomal breakdown of glycogen to glucose, a deficiency of this enzyme is expected to reduce the amount of available intracellular glucose. Moreover, it has been suggested that glucose starvation is involved in the induction of autophagic buildup in the skeletal muscle from the GAA knock-out mice [10]. Indeed, we have demonstrated that normal fibroblasts cultured in low glucose conditions can mimic the suppression of Akt/mTOR signaling in patient fibroblasts (Fig. 2). However, whereas inactivation of Akt was observed in patient fibroblasts cultured with normal glucose-containing medium (Fig. 2), no significant difference in intracellular glucose content between patient and normal fibroblasts was observed (data not shown), suggesting that glucose starvation is not a primary causative factor for Akt suppression in patient fibroblasts. It seems, therefore, that the

induction of autophagy in patient fibroblasts may not purpose to accommodate an energy shortage.

Accumulation of autophagic vacuoles is a critical factor in the resistance of the skeletal muscle to ERT with rhGAA. In the mouse models of Pompe disease, autophagic buildup is known to cause mistargeting of the recombinant enzyme to autophagosomes [5]. Moreover, the successful reversal of lysosomal pathology by ERT has been observed in autophagy-deficient GAA knock-out mice [17]. Suppression of autophagy therefore promises to enhance the therapeutic efficacy of ERT. In this study, we demonstrated that treatment with insulin not only inhibits the accelerated conversion of LC3-I to LC3-II in patient fibroblasts, but also enhances the localization of rhGAA with lysosomes in them (Figs. 3 and 4), suggesting that insulin is an effective drug for suppressing autophagy in patient tissues. Hence, a combination treatment with ERT plus insulin might be a potential therapeutic approach for patients with Pompe disease.

In summary, our results indicate that suppression of Akt mediates the accelerated autophagy observed in fibroblasts from patients with Pompe disease, which is not accompanied by ER stress. The findings also highlight the potential benefit of insulin treatment for improving ERT efficiency.

Conflict of interest disclosures

References

[1] H.G. Hers, alpha-Glucosidase deficiency in generalized glycogenstorage disease (Pompe's disease), Biochem. J. 86 (1963) 11–16.

[2] H.M. van den Hout, W. Hop, O.P. van Diggelen, J.A. Smeitink, G.P. Smit, B.T. Poll-The, H.D. Bakker, M.C. Loonen, J.B. de Klerk, A.J. Reuser, A.T. van der Ploeg, The natural course of infantile Pompe's disease: 20 original cases compared with 133 cases from the literature, Pediatrics 112 (2003) 332–340.

[3] A.T. van der Ploeg, A.J. Reuser, Pompe's disease, Lancet 372 (2008) 1342–1353.

[4] P.S. Kishnani, D. Corzo, M. Nicolino, B. Byrne, H. Mandel, W.L. Hwu, N. Leslie, J. Levine, C. Spencer, M. McDonald, J. Li, J. Dumontier, M. Halberthal, Y.H. Chien, R. Hopkin, S. Vijayaraghavan, D. Gruskin, D. Bartholomew, A. van der Ploeg, J.P. Clancy, R. Parini, G. Morin, M. Beck, G.S. De la Gastine, M. Jokic, B. Thurberg, S. Richards, D. Bali, M. Davison, M.A. Worden, Y.T. Chen, J.E. Wraith, Recombinant human acid [alpha]-glucosidase: major clinical benefits in infantile-onset Pompe disease, Neurology 68 (2007) 99–109.

[5] T. Fukuda, A. Ahearn, A. Roberts, R.J. Mattaliano, K. Zaal, E. Ralston, P.H. Plotz, N. Raben, Autophagy and mistargeting of therapeutic enzyme in skeletal muscle in Pompe disease, Mol. Ther. J. Am. Soc. Gene Ther. 14 (2006) 831–839.

[6] N. Raben, S. Takikita, M.G. Pittis, B. Bembi, S.K. Marie, A. Roberts, L. Page, P.S. Kishnani, B.G. Schoser, Y.H. Chien, E. Ralston, K. Nagaraju, P.H. Plotz, Deconstructing Pompe disease by analyzing single muscle fibers: to see a world in a grain of sand, Autophagy 3 (2007) 546–552.

[7] B. Ravikumar, M. Futter, L. Jahreiss, V.I. Korolchuk, M. Lichtenberg, S. Luo, D.C. Massey, F.M. Menzies, U. Narayanan, M. Renna, M. Jimenez-Sanchez, S. Sarkar, B. Underwood, A. Winslow, D.C. Rubinsztein, Mammalian macroautophagy at a glance, J. Cell Sci. 122 (2009) 1707–1711.

[8] Y. Shimada, H. Kobayashi, S. Kawagoe, K. Aoki, E. Kaneshiro, H. Shimizu, Y. Eto, H. Ida, T. Ohashi, Endoplasmic reticulum stress induces autophagy through activation of p38 MAPK in fibroblasts from Pompe disease patients carrying c.546G>T mutation, Mol. Genet. Metab. 104 (2011) 566–573.

[9] M. Cardone, C. Porto, A. Tarallo, M. Vicinanza, B. Rossi, E. Polishchuk, F. Donaudy, G. Andria, M.A. De Matteis, G. Parenti, Abnormal mannose-6-phosphate receptor trafficking impairs recombinant alpha-glucosidase uptake in Pompe disease fibroblasts, PathoGenetics 1 (2008) 6.

[10] T. Fukuda, L. Ewan, M. Bauer, R.J. Mattaliano, K. Zaal, E. Ralston, P.H. Plotz, N. Raben, Dysfunction of endocytic and autophagic pathways in a lysosomal storage disease, Ann. Neurol. 59 (2006) 700–708.

[11] Y. Shimada, H. Nishida, Y. Nishiyama, H. Kobayashi, T. Higuchi, Y. Eto, H. Ida, T. Ohashi, Proteasome inhibitors improve the function of mutant lysosomal alpha-glucosidase in fibroblasts from Pompe disease patient carrying c.546G>T mutation, Biochem. Biophys. Res. Commun. 415 (2011) 274–278.

[12] E. Fayard, L.A. Tintignac, A. Baudry, B.A. Hemmings, Protein kinase B/Akt at a glance, J. Cell Sci. 118 (2005) 5675–5678.

[13] Z. Yang, D.J. Klionsky, Mammalian autophagy: core molecular machinery and signaling regulation, Curr. Opin. Cell Biol. 22 (2010) 124–131.

[14] R. Zoncu, A. Efeyan, D.M. Sabatini, mTOR: from growth signal integration to cancer, diabetes and ageing, Nat. Rev. Mol. Cell Biol. 12 (2011) 21–35.

[15] X. Xin, Z.A. Khan, S. Chen, S. Chakrabarti, Glucose-induced Akt1 activation mediates fibronectin synthesis in endothelial cells, Diabetologia 48 (2005) 2428–2436.

[16] K. Venkatachalam, S. Mummidi, D.M. Cortez, S.D. Prabhu, A.J. Valente, B. Chandrasekar, Resveratrol inhibits high glucose-induced PI3K/Akt/ERK-dependent interleukin-17 expression in primary mouse cardiac fibroblasts, Am. J. Physiol. Heart Circ. Physiol. 294 (2008) H2078–H2087.

[17] N. Raben, C. Schreiner, R. Baum, S. Takikita, S. Xu, T. Xie, R. Myerowitz, M. Komatsu, J.H. Van der Meulen, K. Nagaraju, E. Ralston, P.H. Plotz, Suppression of autophagy permits successful enzyme replacement therapy in a lysosomal storage disorder–murine Pompe disease, Autophagy 6 (2010) 1078–1089.

[18] T. Katome, T. Obata, R. Matsushima, N. Masuyama, L.C. Cantley, Y. Gotoh, K. Kishi, H. Shiota, Y. Ebina, Use of RNA interference-mediated gene silencing and adenoviral overexpression to elucidate the roles of AKT/protein kinase B isoforms in insulin actions, J. Biol. Chem. 278 (2003) 28312–28323.

[19] J.J. Lum, R.J. DeBerardinis, C.B. Thompson, Autophagy in metazoans: cell survival in the land of plenty, Nat. Rev. Mol. Cell Biol. 6 (2005) 439–448.

[20] A.A. Ellington, M.A. Berhow, K.W. Singletary, Inhibition of Akt signaling and enhanced ERK1/2 activity are involved in induction of macroautophagy by triterpenoid B-group soyasaponins in colon cancer cells, Carcinogenesis 27 (2006) 298–306.

[21] C. Mammucari, G. Milan, V. Romanello, E. Masiero, R. Rudolf, P. Del Piccolo, S.J. Burden, R. Di Lisi, C. Sandri, J. Zhao, A.L. Goldberg, S. Schiaffino, M. Sandri, FoxO3 controls autophagy in skeletal muscle in vivo, Cell Metab. 6 (2007) 458–471.
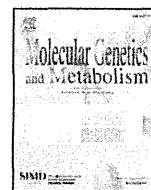
No accumulation of globotriaosylceramide in the heart of a patient with the E66Q mutation in the α-galactosidase A gene

Masahisa Kobayashi [a,*], Toya Ohashi [a,b,g], Takahiro Fukuda [c], Tomoyoshi Yanagisawa [d], Takayuki Inomata [d], Takashi Nagaoka [e], Teruo Kitagawa [f], Yoshikatsu Eto [g], Hiroyuki Ida [a,b,g], Eiji Kusano [h]

[a] Department of Pediatrics, The Jikei University School of Medicine, Tokyo, Japan
[b] Department of Gene Therapy, The Jikei University School of Medicine, Tokyo, Japan
[c] Division of Neuropathology, Department of Pathology, The Jikei University School of Medicine, Tokyo, Japan
[d] Department of Cardio-Angiology, Kitasato University School of Medicine, Kanagawa, Japan
[e] Sagamihara Clinic, Kanagawa, Japan
[f] Tokyo Health Service Association, Tokyo, Japan
[g] Department of Genetic Disease & Genome Science, Jikei University School of Medicine, Tokyo, Japan
[h] Division of Nephrology, Department of Internal Medicine, Jichi Medical University, Tochigi, Japan

ARTICLE INFO

ABSTRACT

Background: Fabry disease is an X-linked lysosomal disorder resulting from mutations in the α-galactosidase A (GLA) gene. Recent reports described that the E66Q mutation of GLA is not a disease-causing mutation. However, no pathological study was reported. We carried out pathological studies using a cardiac biopsy specimen from a patient with the E66Q mutation.
Materials and methods: The case was a 34 year old male patient with end-stage renal failure and cardiomegaly. He was diagnosed with gout at 15 years of age and hemodialysis was started for gouty nephropathy from 31 years of age. He was suspected of having Fabry disease as the result of a screening study for Fabry disease in patients with end-stage renal failure and was referred to our hospital for mutation analysis of the GLA gene. We carried out enzymatic and genetic analysis for GLA and pathological studies of a cardiac biopsy specimen.
Results: The patient had the E66Q mutation in the GLA gene. GLA activity in leukocytes was 36.2% of the average of normal controls. The pathological study of the cardiac biopsy sample showed no characteristic findings of Fabry disease. The immunohistochemistry for GL3 of the cardiac biopsy sample showed no positive cells.
Conclusion: Although the E66Q mutation reduced enzyme activity, the characteristic pathological findings of Fabry disease and the abnormal accumulation of GL3 were not detected in cardiac tissues. The E66Q mutation of the GLA gene is thought to be a functional polymorphism based on enzymatic and pathological studies.

© 2012 Elsevier Inc. All rights reserved.

1. Introduction

Fabry disease (OMIM 301500) is an X-linked lysosomal storage disorder resulting from deficient α-galactosidase A activity (EC 3.2.1.22; GLA) [1]. Its estimated incidence is 1 per 1250–117,000 live male births [1–4]. The deficiency of GLA activity leads to the accumulation of the principal substrate globotriaosylceramide (GL3) in various tissues including vascular endothelium, renal glomeruli and tubules, dorsal root ganglia, cardiac myocytes and valves, cornea and skin.

The residual GLA activity in the leukocytes of male patients with Fabry disease decreases to less than 10% of normal controls and the residual enzymatic activity correlates with the severity of the phenotype. Fabry disease is classified into three clinical forms depending on the severity of the clinical manifestations [1,5–8]. Patients with

classical Fabry disease present with angiokeratoma, acroparesthesias, hypohidrosis, impaired temperature regulation and corneal opacities in childhood or adolescence, and suffer from progressive renal impairment, cardiac hypertrophy, conduction disorder and cerebral vascular events in their second to fifth decade. Patients with the cardiac variant develop cardiac hypertrophy or conduction disorder without other Fabry disease specific manifestations. Patients with the renal variant usually have chronic renal failure and are diagnosed by renal biopsy or screening for Fabry disease. They suffer from renal and cardiac involvement without classical manifestations such as angiokeratoma, acroparesthesias, hypohidrosis and impaired temperature regulation. The renal variant is thought to be an intermediate form between the classical form and the cardiac variant [8].

More than 500 mutations including the E66Q in the GLA gene have been reported. The E66Q mutation in the GLA gene has been reported to be a pathogenic mutation causing atypical Fabry disease [7,9–11], however recently Lee et al. described the E66Q mutation as a functional polymorphism [12]. They reported that the residual GLA activity

* Corresponding author at: 3-25-8 Nishishinbashi Minato-ku, Tokyo 105-8461, Japan.
Fax: +81 3 3435 8665.
E-mail address: masa-koba@jikei.ac.jp (M. Kobayashi).

in leukocytes of patients with the E66Q mutation was 19.0–36.3% of normal controls, and the allele frequency of E66Q mutation in the Korean population was estimated to be 1.046%. To elucidate the pathogenicity of the E66Q mutation of the GLA gene, we carried out pathological studies on a cardiac biopsy specimen from a male patient with the E66Q mutation.

2. Material and methods

2.1. The case

We studied a 34 year old male patient with the E66Q mutation of the GLA gene. He had no positive family history of Fabry disease. He was diagnosed with gout at 15 years of age. The gouty nephropathy developed into end-stage renal failure and hemodialysis was started from 31 years of age. At 34 years of age, a transthoracic echocardiography was performed that showed left ventricular hypertrophy, with the interventricular septum and left ventricular posterior wall thickness of 13 mm and 11 mm respectively. To assess the cause of left ventricular hypertrophy, a cardiac biopsy was carried out. The pathological findings of biopsied tissue did not indicate Fabry disease. However, the patient was suspected to have Fabry disease as a result of a screening study for Fabry disease in patients with end stage renal failure (J-FAST: Japan Fabry disease screening study) and was referred to our hospital for enzymatic and genetic analysis of GLA and immunohistochemistry using monoclonal anti-GL3 antibody at the age of 35 years. He had no characteristic symptoms of Fabry disease other than end-stage renal failure and cardiomegaly.

2.2. Enzymatic analysis

Leukocytes were extracted from heparinized whole blood from the patient and GLA activity in leukocytes was analyzed using a fluorogenic substrate, 4-methylumbelliferyl-α-D-galactopyranoside, as described previously [13]. As controls, enzymatic activity in leukocytes from normal subjects (n = 3) and from male patients with classical Fabry disease (n = 47) was also assayed.

2.3. Genetic analysis

Genomic DNA was extracted from leukocytes using blood and cell culture DNA midi kit (Qiagen, Jilden, Germany). Each exon and flanking intron sequence of the GLA gene was amplified by PCR using AmpliTaq gold 360 master mix (Applied Biosystems, Foster city, CA, USA), and directly sequenced using the BigDye Terminator kit, version 3.1 (Applied Biosystems, Foster city, CA, USA).

2.4. Pathological studies using a cardiac biopsy specimen

A light microscopic study (hematoxylin and eosin and Masson's trichrome stain), an immunohistochemistry using monoclonal anti-GL3 antibody (Seikagaku Corp, Chiyoda-ku, Tokyo, Japan), and an electron microscopic study were carried out using the patient's cardiac biopsy specimen. As a positive control, a cardiac biopsy specimen from a 31 year old male patient with classical Fabry disease was also studied.

This study was performed under the approval of the ethical committee of the Jikei University School of Medicine.

3. Results

3.1. Enzymatic analysis (Fig. 1)

The mean GLA activity of normal controls was 131.3 nmol/mg/h (101.7–160.8 nmol/mg/h). The residual GLA activity of the present case and patients with classical Fabry disease were 47.73 nmol/mg/h (36.3% of normal control) and 2.7 ± 3.4 nmol/mg/h (2.1 ± 2.6 of normal control (mean ± SD)) respectively. Although the present case's GLA activity was lower than normal controls, the residual GLA activity was higher than that of classical Fabry patients.

3.2. Genetic analysis

A missense mutation E66Q (C196 G>C) was detected on exon 2 in the GLA gene. There was no mutation in any other exon and flanking intron sequence.

3.3. Pathological studies using cardiac biopsy specimen

3.3.1. Light microscopic study

3.3.1.1. Hematoxylin and eosin (HE) stain (Fig. 2). The characteristic pathological finding of Fabry disease using HE stain is vacuolated myocardial cells which indicate the accumulation of GL3 in these cells. Although the pathological findings of the classical Fabry patient showed the numerous vacuolated myocardial cells (arrows, Fig. 2A), there were no characteristic pathological findings for Fabry disease in cardiac tissue from the present case (Fig. 2B).

Normal controls : 101.7~160.8 nmol/mg/hr (mean 131.3 nmol/mg/hr)
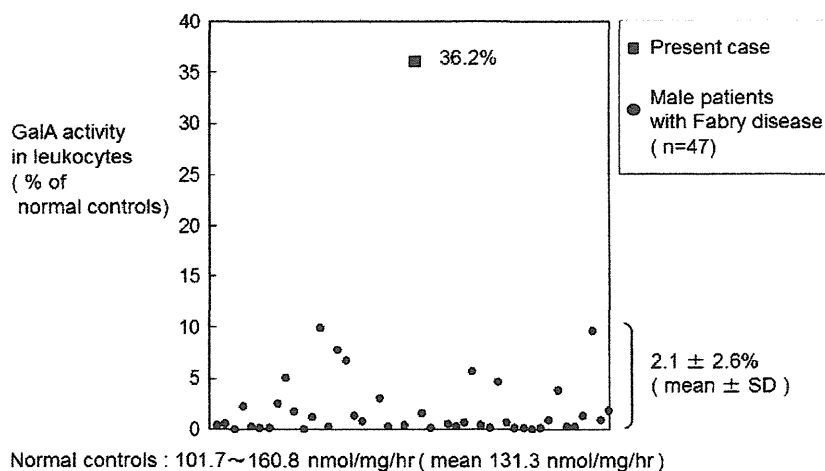
Fig. 1. The result of enzymatic analysis. The mean residual leukocyte GLA activity of the patients with classical Fabry disease was 2.7 ± 3.4 nmol/mg/h (2.1 ± 2.6% (mean ± SD) of normal controls). The residual leukocyte GAL activity of the present case was 47.73 nmol/mg/h (36.3% of normal controls).
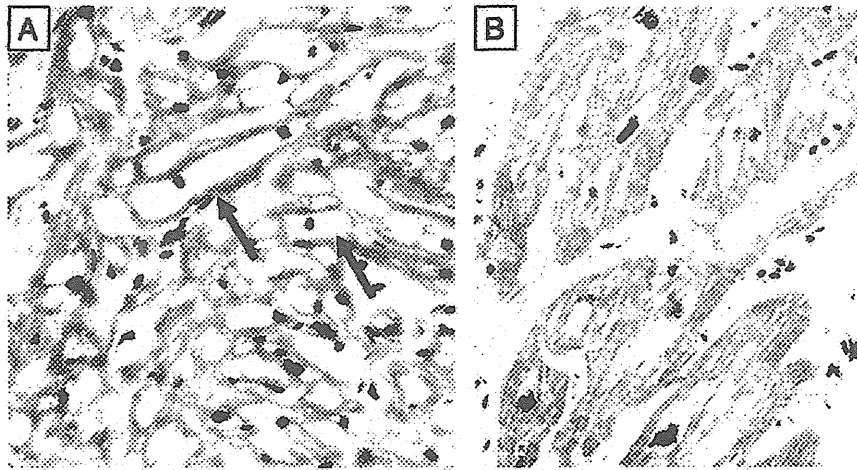
Fig. 2. HE stain of the cardiac biopsy specimens of a male patient with classical Fabry disease and the present case. Although the pathological findings of the classical Fabry patient showed numerous vacuolated myocardial cells (arrows, A), there were no characteristic pathological findings for Fabry disease in cardiac tissue from the present case (B).

3.3.1.2. Masson's trichrome stain (Fig. 3). The characteristic pathological findings of Fabry disease using Masson's trichrome stain are vacuolated myocardial cells and cardiac fibrosis with fibrous change around myocardial cells. Although cardiac fibrosis was shown in both classical Fabry patients and the present case (Figs. 3A and B), numerous vacuolated myocardial cells (arrows in Fig. 3A) were detected in only classical Fabry patients.

3.3.1.3. Immunohistochemistry using monoclonal anti-GL3 antibody (Fig. 4). GL3 positive myocardial cells indicate accumulation of GL3. Although there were numerous GL3 positive myocardial cells (arrows) in cardiac tissue from the classical Fabry patient (Fig. 4A), there were no GL3 positive myocardial cells in cardiac tissue from the present case (Fig. 4B).

3.3.2. Electron microscopic study

The characteristic pathological finding of Fabry disease in electron microscopic studies is zebra bodies, which indicate the accumulation of GL3 in myocardial cells. Although zebra bodies (arrows) were seen in myocardial cells from the classical Fabry patient (Fig. 5A), there were no zebra bodies in cardiac tissue from the present case (Fig. 5B).

4. Discussion

Recently, screening for Fabry disease in end-stage renal disease patients was carried out by several groups and the detected Fabry

disease patients at various incidences [3,4,7,10,11,14]. With the exception of one report that the combination mutation of E66Q and R112C was found in patients with classical Fabry disease [9], E66Q has been identified from screening for Fabry disease [7,10,11]. Because the method of screening for Fabry disease was measurement of the GLA activity, some patients were thought to be misdiagnosed without clinical and pathological evaluation. It was reported that the residual GLA activity of patients with the E66Q mutation is higher than with any other mutation. However, there is no clear evidence of GL3 accumulation in tissues.

Lee et al. studied 1176 alleles in the Korean population and the E66Q mutation in the GLA gene was detected in 12 alleles. They estimated that the allele frequency with E66Q mutation in the Korean population was 1.046% and concluded that the E66Q mutation is a functional polymorphism. Even in their study, there was no pathological evaluation. To conclude that the E66Q mutation is a functional polymorphism, pathological study, particularly focusing on GL3 accumulation, is necessary.

In this study, we carried out enzymatic, genetic and pathological studies on a patient with the E66Q mutation of the GLA gene. The mean residual leukocyte GLA activity level of classical Fabry patients was 2.1 ± 2.6% of normal controls. However, the leukocyte GLA activity level of the present case decreased by 36.3% of normal controls and was higher than that of the classical Fabry patients. The activity reduction due to the E66Q mutation might not be enough to cause GL3 accumulation in tissues. In this regard, the pathological studies
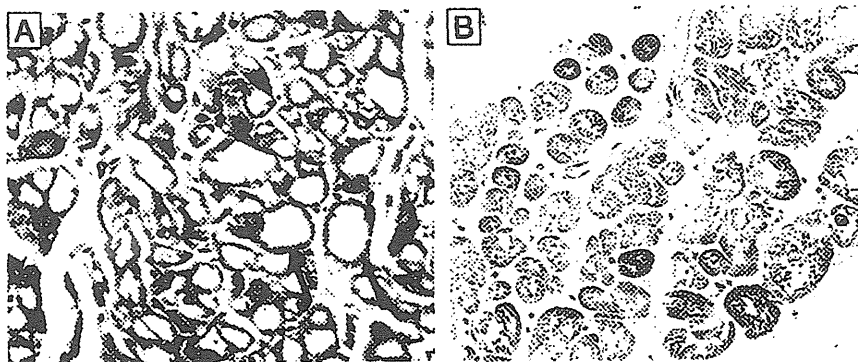
Fig. 3. Masson's trichrome stain of cardiac biopsy specimens of a male patient with classical Fabry disease and the present case. Although cardiac fibrosis was shown in both classical Fabry patient and the present case (A and B), numerous vacuolated myocardial cells (arrows in A) were detected only in the classical Fabry patient. In the present case there were no characteristic pathological findings for Fabry disease in cardiac tissue from the present case (B).
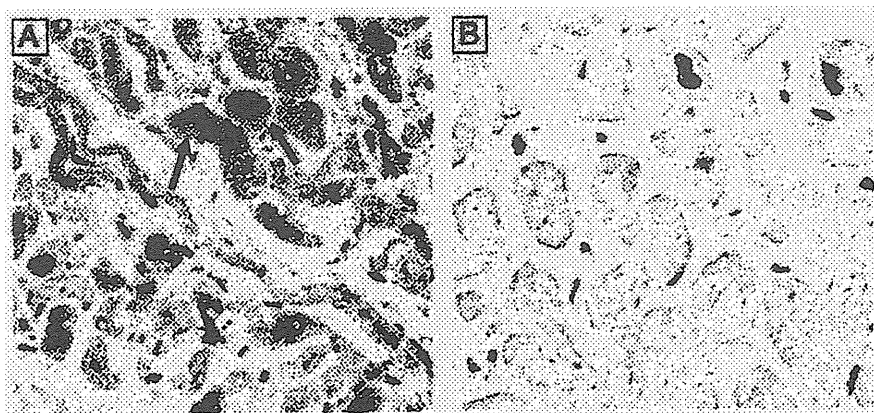
Fig. 4. Immunohistochemistry using monoclonal anti-GL3 antibody of cardiac biopsy specimens of a male patient with classical Fabry disease and the present case. Although there were numerous GL3 positive myocardial cells (arrows) in cardiac tissue from the classical Fabry patient (A), there were no GL3 positive myocardial cells in those from the present case (B).

on the cardiac biopsy specimen of the present case showed no characteristic findings for Fabry disease, such as vacuolated myocardial cells on light microscopic study or zebra bodies on electron microscopic study. We carried out immunohistochemistry using monoclonal anti-GL3 antibody to evaluate the accumulation of GL3 in myocardial cells. Although GL3 positive cells were detected in previously diagnosed Fabry patients, they were not detected in the present case. These findings suggest that the E66Q mutation in the GLA gene does not lead to the accumulation of GLA in myocardial cells. Left ventricular hypertrophy and cardiac fibrosis are common complications among patients with chronic kidney disease and end stage renal failure treated with hemodialysis [14]. The echocardiography and the pathological studies on the cardiac biopsy specimen of the present case showed left ventricular hypertrophy and cardiac fibrosis respectively and likely represent complications of hemodialysis. Therefore, we conclude that the E66Q mutation in the GLA gene is a functional polymorphism based on enzymatic and pathological studies.

Gaspar et al. studied hemodialysis patients and found 1 male and 1 female patient with the D313Y mutation in the GLA gene [15]. The residual leukocyte GLA activity of the male patient with the D313Y mutation was 39% of control mean and the D313Y mutation was reported as a "pseudo-deficiency" mutation [16]. There might be polymorphisms other than E66Q mutation and it would be more cautious to diagnose asymptomatic cases found by screening for Fabry disease.

There are some limitations in this study. We studied only one patient with the E66Q mutation and the pathological studies were

performed only on a cardiac biopsy specimen. To further support the idea that the E66Q mutation in this patient is a functional polymorphism, a renal biopsy could be helpful because the patient has end-stage renal disease. However he has received hemodialysis for 3 years and his renal tissues are likely to have been replaced by scars making a renal biopsy problematic.

5. Conclusion

The E66Q mutation in the GLA gene was thought to be a functional polymorphism and physicians should be cautious when making a Fabry diagnosis in patients with the E66Q mutation.

Conflict of interest

T. Ohashi, Y. Eto and H. Ida have active research support from Genzyme Corporation. These activities have been fully disclosed and are managed under Memorandum of Understanding with the Conflict of Interest Resolution Board of the Jikei University School of Medicine.

References

[1] R.J. Desnick, Y.A. Ioannou, C.M. Eng, α-Galactosidase A deficiency: Fabry disease, in: C.R. Scriver, A.L. Beaudet, W.S. Sly, D. Valle (Eds.), The Metabolic and Molecular Basis of Inherited Disease, 8th ed., McGraw-Hill Inc, New York, 2001, pp. 3733–3774.
[2] P.J. Meikle, J.J. Hopwood, A.E. Clague, W.F. Carey, Prevalence of lysosomal storage disorders, JAMA 281 (1999) 249–254.
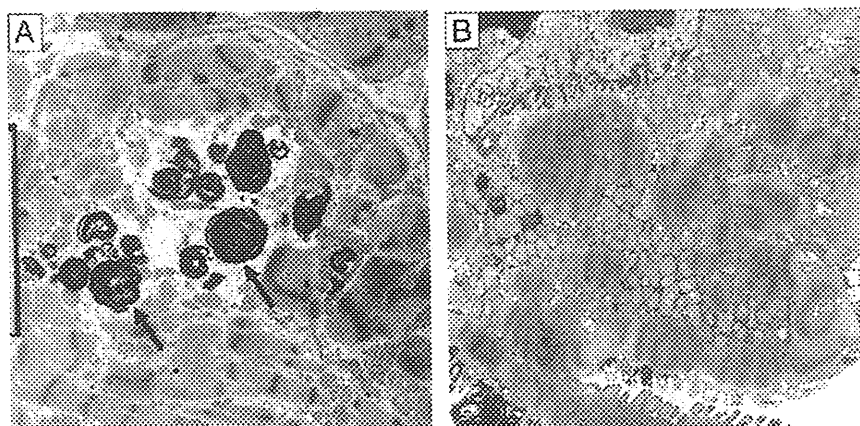
Fig. 5. Electron microscopic study of cardiac biopsy specimens of a male patient with classical Fabry disease and the present case. Although zebra bodies (arrows) were seen in myocardial cells from the classical Fabry patient (A), there were no zebra bodies in those from the present case (B).

[3] M. Spada, S. Pagliardini, M. Yasuda, T. Tukel, G. Thiagarajan, H. Sakuraba, A. Pnonzone, R.J. Desnick, High incidence of later onset Fabry disease revealed by newborn screening, Am. J. Hum. Genet. 79 (2006) 21–40.

[4] W.L. Hwu, Y.H. Chien, N.C. Lee, S.C. Chiang, R. Dobrovolny, A.C. Huang, H.Y. Yeh, M.C. Chao, S.H. Lin, T. Kitagawa, R.J. Desnick, L.W. Hsu, Newborn screening for Fabry disease in Taiwan reveals a high incidence of the later-onset GLA mutation c.936 + 919G>A (IVS4 + 919G>A), Hum. Mutat. 30 (2009) 1397–1405.

[5] S. Ishii, R. Kase, H. sakuraba, Y. Suzuki, Characterization of a mutant alpha-galactosidase gene product for the late-onset cardiac form of Fabry disease, Biochem. Biophys. Res. Commun. 197 (1993) 1585–1589.

[6] S. Nakao, T. Takenaka, M. Maeda, C. Kodama, A. Tanaka, M. Tahara, A. Yoshida, M. Kuriyama, H. Hayashibe, H. Sakuraba, H. Tnaka, An atypical variant of Fabry's disease in men with left ventricular hypertrophy, N. Engl. J. Med. 333 (1995) 288–293.

[7] S. Nakao, C. Kodama, T. Takenaka, A. Tanaka, Y. Yasumoto, A. Yoshida, T. Kanzaki, A.L.D. Enriquez, C.M. Eng, H. Tanaka, C. Tei, R.J. Desnick, Fabry disease: detection of undiagnosed hemodialysis patients and identification of a "renal variant" phenotype, Kidney Int. 64 (2003) 801–807.

[8] R.J. Desnick, M. Banikazemi, M. Wasserstein, Enzyme replacement therapy for Fabry disease, an inherited nephropathy, Clin. Nephrol. 57 (2002) 1–8.

[9] T. Okumiya, S. Ishii, T. Takenaka, R. Kase, S. Kamei, H. Sakuraba, Y. Suzuki, Galactose stabilized various missense mutants of α-galactosidase in Fabry disease, Biochem. Biophys. Res. Commun. 214 (1995) 1219–1224.

[10] M. Tanaka, T. Ohashi, M. Kobayashi, Y. Eto, N. Miyamura, K. Nishida, E. Araki, K. Itoh, K. Matsushita, M. Hara, K. Kuwahara, T. Nakano, N. Yasumoto, H. Nonoguchi, K. Tomita, Identification of Fabry's disease by the screening of α-galactosidase A activity in male and female hemodialysis patients, Clin. Nephrol. 64 (2005) 281–287.

[11] H. Fujii, K. Kono, S. Goto, T. Onishi, H. Kawai, K. Hirata, K. Hattori, K. Nakamura, F. Endo, M. Fukagawa, Prevalence and cardiovascular features of Japanese hemodialysis patients with Fabry disease, Am. J. Nephrol. 30 (2009) 527–535.

[12] B.H. Lee, S.H. Heo, G.H. Kim, J.Y. Park, W.S. Kim, D.H. Kang, K.H. Choe, W.H. Kim, S.H. Yang, H.W. Yoo, Mutations of the GLA gene in Korean patients with Fabry disease and frequency of the E66Q allele as a functional variant in Korean newborns, J. Hum. Genet. 55 (2010) 512–517.

[13] R.J. Desnick, K.Y. Allen, S.J. Desnick, M.K. Raman, R.W. Bemlohr, W. Krivit, Fabry's disease: enzymatic diagnosis of hemizygotes and heterozygotes. Alpha-galactosidase activities in plasma, serum, urine and leukocytes, J. Lab. Clin. Med. 81 (1973) 157–171.

[14] R. Glassock, R. Pecoits-Filho, S.H. Barberato, Left ventricular mass in chronic kidney disease and ESRD, Clin. J. Soc. Nephrol. 4 (2009) S79–S91.

[15] P. Gaspar, J. Herrera, D. Rodrigues, S. Cerezo, R. Delgado, C.F. Andrade, R. Forascepi, J. Macias, M.D. del Pino, M.D. Prados, P.R. de Alegria, G. Torres, P. Vidau, M.C. Sa-Miranda, Frequency of Fabry disease in male and female haemodialysis patients in Spain, BMC Med. Genet. 11 (2010) 11–19.

[16] R. Froissart, N. Guffon, M.T. Vanier, R.J. Desnick, I. Maire, Fabry disease: D131Y is an alpha-galactosidase A sequence variant that causes pseudodeficient activity in plasma, Mol. Genet. Metab. 80 (2003) 305–314.

XII ライソゾーム病

ゴーシェ病
Gaucher disease

Key words：ゴーシェ病，酵素補充療法，ライソゾーム病

井田博幸

1. 疾患概念

ゴーシェ病はライソゾーム酵素であるグルコセレブロシダーゼ活性低下により発症するライソゾーム病である．肝脾腫を主症状とし，神経症状の有無とその重症度により1型(慢性非神経型，成人型)，2型(急性神経型，乳児型)，3型(亜急性神経型，若年型)に臨床分類されている．このような臨床的異質性が存在するが，更にこれら各病型内においても種々の表現型の差異が存在するのが本症の特徴である．

2. 疫学

ユダヤ人に好発し，その頻度は約1,000人に1人である．日本人では50万〜100万人に1人

と報告されている．1992年から現在までに当科で診断されたゴーシェ病は約130人である．

3. 病因

グルコセレブロシダーゼの遺伝的酵素活性低下により，その基質であるグルコセレブロシドが主として肝臓，脾臓，骨髄などの細網内皮系に蓄積することによって発症する．神経症状はグルコセレブロシドのリゾ体であるグルコシルスフィンゴシンの脳内蓄積により引き起こされる．その病態生理を図1にまとめる．

4. 臨床症状

前述したように神経症状の有無とその重症度により，臨床上，1型，2型，3型に分類されて

ライソゾーム病

図1 ゴーシェ病の基本病態

Hiroyuki Ida: Department of Pediatrics, Jikei University School of Medicine　東京慈恵会医科大学 小児科
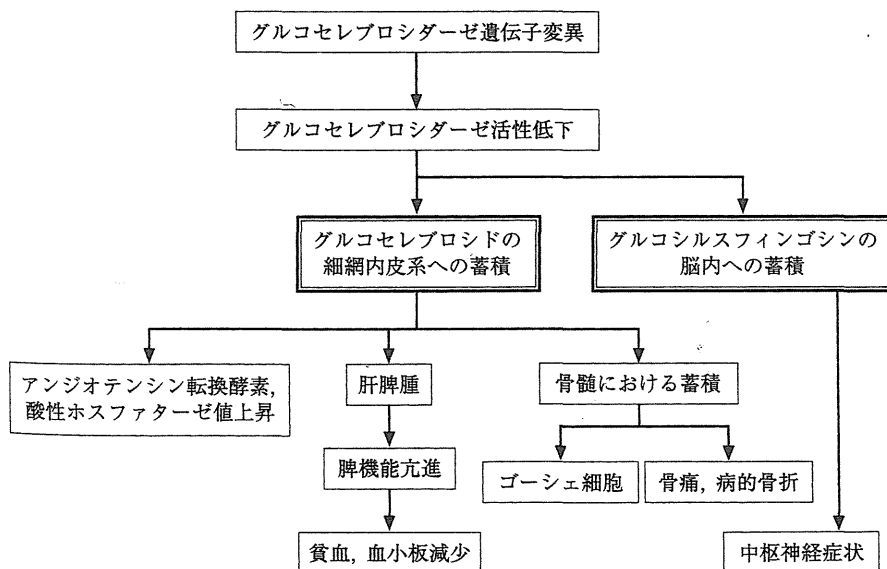
表1　ゴーシェ病の臨床病型

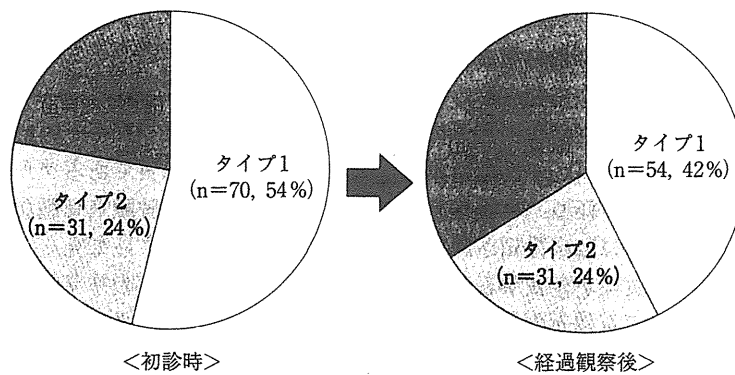|	1型 慢性非神経型	2型 急性神経型	3型 亜急性神経型
発症時期	幼児〜成人	乳児	乳児〜学童
神経症状	(−)	(＋＋＋)	(＋)〜(＋＋)
肝脾腫	(−)〜(＋＋＋)	(＋)	(＋)〜(＋＋＋)
骨症状	(−)〜(＋＋＋)	(−)	(−)〜(＋＋＋)
予後	良好	不良	症例により異なる

図2　日本人ゴーシェ病の病型変化(n＝129)

いる. これら病型により経過, 予後は異なる(表1). 自験例による129例のデータでは日本人ゴーシェ病は1型が42％, 2型が24％, 3型が34％と神経型ゴーシェ病の頻度が高いことが特徴である(経過観察後のデータによる).

1型は神経症状を伴わない病型で肝脾腫, 血小板減少, 骨症状を主症状とする. 発症年齢, 骨合併症の有無, 肝脾腫の程度などの点において臨床的異質性が顕著な病型である. ユダヤ人では極めて慢性に経過するが, 日本人では進行性であることが明らかにされている. 我が国において酵素補充療法を行っている経過中に神経症状を呈し, 3型に再分類される例が1型の約20％報告されているので, 1型と診断されても異常眼球運動や精神運動発達遅滞などの神経症状の発症に注意する(図2). これら1型から3型に移行する症例においてはL444P/L444P, L444P/F213Iという遺伝子型が高頻度に認められる[1].

2型は乳児期に発症し, 肝脾腫に加えて痙攣, 後弓反張, 喉頭痙攣, 異常眼球運動などの神経症状を呈し, これら神経症状が急速に進行する病型である. 2型の最重症型として胎児水腫・コロジオンベビーとして発症する新生児型も存在する[2].

3型は肝脾腫に加えて神経症状を伴うが, その発症は2型に比較して遅く, またその程度や進行も緩徐な病型である. 3型は3a, 3b, 3cの亜型に分類されている. 3a型は古典的な3型で肝脾腫に加えて痙攣, ミオクローヌス, 小脳失調, 眼球運動失行などの神経症状を呈する. 3b型は核上性上方注視麻痺を唯一の神経症状とし, それに加えて重篤な臓器症状(巨大脾腫, 骨折・骨痛, 呼吸器症状など)を呈する病型である. 早期発症の1型との鑑別が困難な病型である[3]. 3c型は水頭症, 角膜混濁, 心弁膜石灰化などユニークな臨床症状を呈する病型である[4].

5. 診断と鑑別診断

肝脾腫と血小板減少を認めた場合, 骨髄穿

を行い腫瘍性疾患が否定されて，かつゴーシェ細胞が存在すれば診断はほぼ確実である．酸性ホスファターゼ値の上昇，アンジオテンシン変換酵素値の上昇などの所見は本症の診断を支持する．確定診断は培養皮膚線維芽細胞のグルコセレブロシダーゼ活性低下を証明することによってなされる．通常，酵素活性は正常の10％以下である．出生前診断は培養羊水細胞のグルコセレブロシダーゼ活性測定により可能である．鑑別診断としてはNiemann-Pick病A型，B型があるが，骨髄中のNiemann-Pick細胞の存在やスフィンゴミエリナーゼ活性測定により鑑別が可能である．Niemann-Pick病C型は培養皮膚線維芽細胞のフィリピン染色により鑑別が可能である．遺伝子診断は遺伝子変異の集積性が高いユダヤ人では有用であるが，日本人においてはL444P変異が約35％，F213I変異が約15％でcommon mutationのスクリーニングで同定できない変異が約40％存在するため，その有用性は低い[5]．

6. 治療と予後

治療法としては我が国では酵素補充療法と骨髄移植が実地臨床上行われている．1型に対してこれら治療は有効でありその予後は良好である．これに対して2型に対する酵素補充療法や骨髄移植の有効性は乏しく，2型の予後は不良である．3型に対する酵素補充療法は神経症状が重篤でない症例のみに有効である．診断時に神経症状を呈する3型は一般的に酵素補充療法に抵抗性で予後は不良である．これに対して1型から3型に移行した症例では酵素補充療法により生命的予後は比較的良好であるが，神経症状の改善は認められない．

酵素補充療法としてはグルコセレブロシダーゼcDNAをCHO(Chinese hamster ovary)細胞に導入して作製した酵素製剤(商品名：セレザイム®)が現在，我が国で用いられている．日本ではすべての病型に適応が認められており，初期投与量として病型，年齢にかかわらず1回60単位/kgを2週間ごとに点滴静注する．症状の改善により投与量は漸減できるが骨症状の改善には初期投与量を少なくとも2年間，継続することが推奨されている．この骨症状の評価には単純X線では不十分で，大腿骨頭から膝関節を含めたMRIが必須である．安易な酵素量の減量は骨症状の発症をきたすので注意する[6]．

骨髄移植は1型にも適応はあるが酵素補充療法が有効かつ安全なので，1型に対しては第一選択ではない．欧米において3型に対する報告が散見される．それによると肝脾腫，血液学的異常，低身長の改善のみならず神経症状の進行停止が認められている[7]．したがって，その危険性や侵襲を考えると，骨髄移植の適応は酵素補充療法を行っても神経症状が進行する全身状態の良好な症例である．

ライソゾーム病

■文　献

1) Tajima A, et al: Clinical and genetic study of Japanese patients with type 3c Gaucher disease. Mol Genet Metab **97**: 272-277, 2009.
2) Mignot C, et al: Perinatal-lethal Gaucher disease. Am J Med Genet **120A**: 338-344, 2003.
3) Patterson MC, et al: Isolated horizontal supranuclear gaze palsy as a marker of severe involvement in Gaucher's disease. Neurology **43**: 1993-1997, 1993.
4) Abrahamov A, et al: Gaucher's disease variant characterized by progressive calcification of heart valves and unique genotype. Lancet **346**: 1000-1003, 1995.
5) Ida H, et al: Mutation prevalence among 47 unrelated Japanese patients with Gaucher disease: identification of four novel mutations. J Inherit Metab Dis **20**: 67-73, 1997.
6) Ida H, et al: Severe skeletal complications in Japanese patients with type 1 Gaucher disease. J Inherit Metab Dis **22**: 63-73, 1999.
7) Malatack JJ, et al: The status of hematopoietic stem cell transplantation in lysosomal storage disease. Pediatr Neurol **29**: 391-403, 2003.
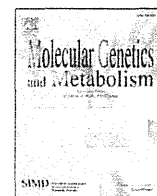
Brief Communication

Genistein reduces heparan sulfate accumulation in human mucolipidosis II skin fibroblasts

Takanobu Otomo *, Mohammad Arif Hossain, Keiichi Ozono, Norio Sakai

Department of Pediatrics, Osaka University Graduate School of Medicine, 2-2 Yamada-oka, Suita, Osaka 565-0871, Japan

ARTICLE INFO

ABSTRACT

Genistein, a soy isoflavone, reduces glycosaminoglycan synthesis and its effect on mucopolysaccharidoses has been tested. In this report, we examined the effect of genistein in human mucolipidosis II skin fibroblasts in vitro. Heparan sulfate was accumulated within both cells and in extracellular spaces in mucolipidosis II. Genistein reduced the amount of heparan sulfate in cultured cells dose dependently and also inhibited cell growth dose dependently.

© 2011 Elsevier Inc. All rights reserved.

1. Introduction

Mucolipidosis II (ML-II) (MIM #252500) is an autosomal recessive lysosomal storage disorder caused by the deficiency of GlcNAc-phosphotransferase (UDP-N-acetylglucosamine-lysosomal-enzyme N-acetylglucosaminephosphotransferase; EC 2.7.8.17), which generates mannose 6-phosphate (M6P) recognition markers on lysosomal acid hydrolases [1]. As a result, almost all lysosomal acid hydrolases are no longer targeted to lysosomes and massive accumulation occurs within lysosomes, which are observed as "inclusion bodies". These inclusion bodies are composed of accumulations such as saccharides, proteins, cholesterol, phospholipids, and glycosaminoglycan (GAG).

Genistein is a soy isoflavone, which is found in various foods made from soybeans. Genistein has been reported to reduce GAG synthesis [2] and improves neurodegenerative disorders such as mucopolysaccharidoses (MPS) [3]. However, the specific effect of genistein on ML-II cells has not been reported so far. In this report, we investigated the in vitro effect of genistein in cultured skin ML-II fibroblasts.

2. Materials and methods

2.1. Skin fibroblasts and cell culture

We obtained skin fibroblasts from a healthy subject and three ML-II patients after obtaining written informed consent. Mutations in the GNPTAB gene were c.3565C>T(p.R1189X)/c.3565C>T(p.R1189X), c.310C>T(p.Q104X)/c.3428_3429insA(p.N1143fs), and c.310C>T(p.Q104X)/c.2544delA(p.K848fs) in the respective ML-II cell lines [4]. We also purchased two normal skin fibroblast cell lines (HDFn from Invitrogen and NHDF from Lonza). Cells were cultured using standard methods with Dulbecco's Modified Eagle Medium (Gibco) plus 10% fetal bovine serum (Sigma) and Antibiotic–Antimycotic (Gibco). Genistein (Sigma) was dissolved in dimethyl sulfoxide (DMSO): the total amount of DMSO added to culture media remained the same (0.1% concentration in culture medium) and only genistein concentration varied in this study.

2.2. Immunofluorescence staining

Cells were fixed with 3.7% formaldehyde for 1 h followed by permeabilization with 0.1% Triton-X100 for 15 min and blocking with 1% bovine serum albumin for 1 h at room temperature. Cells were treated with mouse anti-heparan sulfate (HS) monoclonal antibody (10E4; Seikagaku Biobusiness) at 1:100 for 1 h followed by staining with Alexa Fluor 488 (Molecular Probes) at 1:1000 for 1 h at room temperature. Finally, cells were stained with 4′,6-diamidino-2-phenylindole (DAPI) (Dojindo) at 1:1000 for 15 min at room temperature and mounted on slides. Fluorescence images were acquired using a fluorescence microscope (BX51; Olympus).